Ferreiro, Javier Ojea; Gregori, Wildmer Daniel; Nardo, Michela

Working Paper

Forecasting M&A deals with MIDAS count model

JRC Working Papers in Economics and Finance, No. 2022/15

Provided in Cooperation with:
Joint Research Centre (JRC), European Commission

Suggested Citation: Ferreiro, Javier Ojea; Gregori, Wildmer Daniel; Nardo, Michela (2022) : Forecasting M&A deals with MIDAS count model, JRC Working Papers in Economics and Finance, No. 2022/15, European Commission, Ispra

This Version is available at:
https://hdl.handle.net/10419/283078

European Commission

JRC TECHNICAL REPORT

Forecasting M&A deals with MIDAS count model

Ojea Ferreiro, Javier.

Gregori, Wildmer Daniel

Nardo, Michela

2022

JRC Working Papers in Economics and Finance, 2022/15

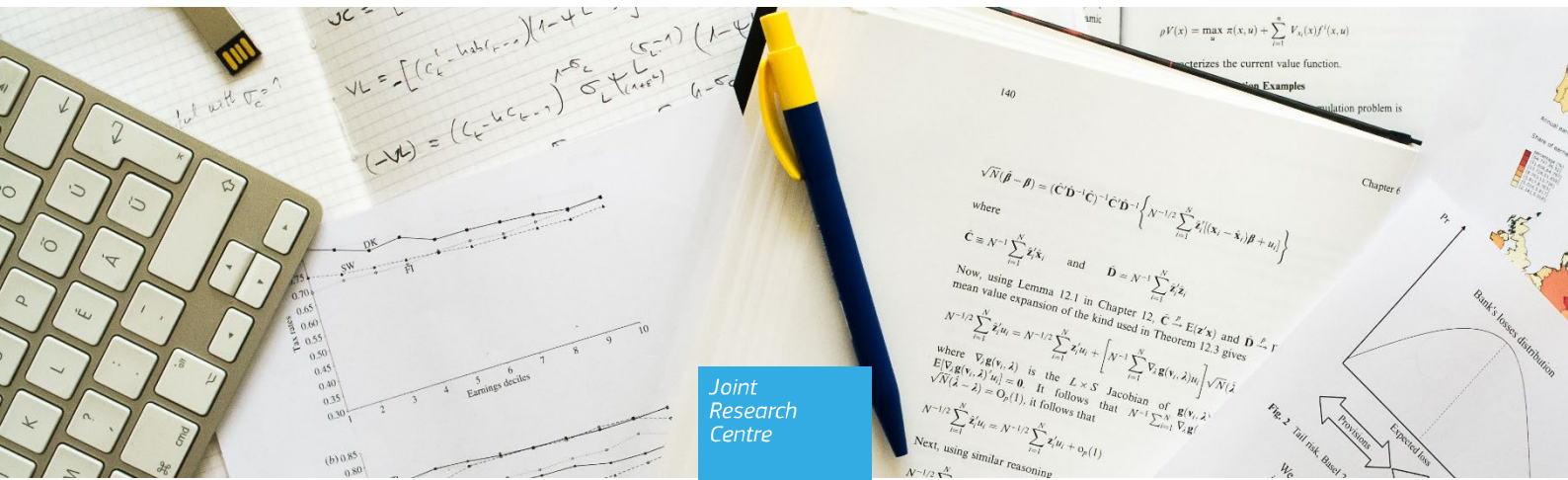

Contact information
Name: Michela Nardo
Email: michela.nardo@ec.europa.eu

EU Science Hub
https://joint-research-centre.ec.europa.eu

JRC130234

Ispra, European Commission, 2022

How to cite this report: Ojea Ferreiro, J., Gregori, W. D., and Nardo, M., *Forecasting M&A deals with MIDAS count model*, European Commission, 2022, JRC130234

Forecasting M&A deals with MIDAS count model

(this version: July 2022) [1]

Abstract

This report focuses on the forecast of the number of monthly cross-border deals in the European Union. We propose a new model to improve the forecasting properties of a count model of Foreign Direct Investment deals in EU, by taking into account past trends in high-frequency (daily) deal data and the decomposition of the conditional overdispersion into short-term and long-term components. Our model relies on the dynamic behaviour of the first two moments of the distribution of FDI deals to explain the evolution of parameters η and π in the Negative Binomial distribution. We test this model with several subsets of M&A deals from 1998 to 2021 obtaining sizable forecast improvements as compared to benchmark INGARCH models.

Keywords: M&A forecasting, MIDAS approach, count process, overdispersion

JEL codes: C10, C19, C35

[1] We would also like to thank participants at ECFIN-JRC seminar and the 2020/2021 Italian Society of Applied and Industrial Mathematics (SIMAI) Responsibility for any errors lies solely with the authors. The views expressed are purely those of the authors and may not in any circumstances be regarded as stating an official position of the European Commission.

Non-technical summary

This paper proposes a negative binomial model to forecast M&A deals where both parameters are time-varying. To capture early trends in the future evolution of the count time series we use high frequency data (MIDAS) which update the estimation of the two first moments, i.e. mean and variance. The MIDAS approach allows us to decompose the variance in a long and short term component.

The variable to be forecasted in this study is the monthly number of inbound M&A in the European Union, i.e. the number of M&A transactions with investors located outside the EU. The data sample begins in 1998 and ends in the first quarter of 2021.

We analyse the forecasted distribution and the point forecasts of our model in comparison with benchmark models to forecast inbound M&A deals in EU at aggregate, regional and sectorial levels. Results suggest that our model improve the previous approaches on different dimensions, especially in terms of the overall forecasted distribution but also in the point estimate forecast.

1. Introduction

This paper focuses on the estimation of a count model of the number of cross-border deals in the European Union, where the first and second moments of the count variable are modelled by observing the dynamics in the high frequency (daily) data. We distinguish the stochastic trend of the count model from the overdispersion in the count process, modelled with high frequency data. The contemporaneous use of a count model and high frequency data allows to improve the forecasting performance of the model significantly as it permits to eliminate the excess volatility presented in the short-term forecasts. We check the performance of our model with standard benchmark measures and add exogenous variables on cross-border M&A determinants to further improve the forecasting performance.

The main motivation to forecast the number of deals is the need to have a reliable prediction of the number of transactions to be screened by public authorities. As of July 2021, 18 European countries have a national FDI screening mechanism in place, adopted a new national FDI screening mechanism, or are in the process to adopt one[2]. Additionally, the European Commission has the possibility to express an opinion for every foreign investment which is likely to constitute a threat for security or public order in EU (Regulation 452/2019)[3]. The screening implies, for European countries and the Commission services, a constant flow of notifications to evaluate. The possibility to predict in advance the number of deals is therefore of great help when organising internally the screening activities. This study is the first attempt to produce such a forecast for all EU countries.

Additional reasons motivate this work. On the one hand the need to proxy future cross-border capital inflows overcoming the first-counterpart principle used to collect official FDI statistics[4] as our M&A deals are classified according to the jurisdiction of the ultimate controlling parent. The reliable forecast of the number of inbound M&A deals in the EU would in fact constitutes a valuable proxy of the influence exerted by some countries, such as China, that massively use offshores or shell companies outside China to invest in EU. On the other hand, during the Covid-19 shock and in its aftermath, vulnerable EU companies in certain sectors (e.g. in pharmaceuticals) were subject to hostile takeovers or minority investments by foreign investors (OECD, 2020a; OECD, 2020b). Forecasting the likely

[2] European Commission, 2021. Reports from the commission to the European parliament and the Council first annual report on the screening of foreign direct investments into the union and report on the implementation of regulation. Publications Office of the European Union, Luxembourg (EU) 2021/821.

[3] See: https://eur-lex.europa.eu/eli/reg/2019/452/oj.

[4] Official FDI statistics (flows and stocks) hosted in the National Accounts are collected according to the first-counterpart principle. Therefore, if a Chinese company uses a subsidiary in Luxembourg to acquire a firm in Spain, the FDI data will record twice the transaction, once as transaction between China and Luxembourg and the second as transaction between Luxembourg and Spain.

number of deals in these sectors is helping to devise anomalous behaviours and spot increasing foreign attention towards vulnerable sectors.

The literature on M&A deals has actually used count models to identify and analyse the determinants of M&A. However, the use of these models to produce forecasts is an absolute novelty of this paper. Hijzen et al. (2008) for example, use a negative binomial regression to study whether the determinants of the M&A deals (especially those related to distance and trade policy barriers) may have a different impact on the actual number of deals depending on the type of merger, i.e. horizontal or vertical. Pozzolo and Focarelli (2008) employ a negative binomial regression to analyse the determinants of cross-border M&As in the banking and insurance sectors with the aim to explain the different degree of internationalization of these two sectors. Bertrand et al. (2005) instead, for a set of 18 OECD countries, compare different Poisson and negative binomial models to study how the location of production plants affects the number of cross-border M&A deals in different sectors. Girma (2002) uses a count model for the number of foreign-acquired plants to analyse to what extent the abolition of all existing non-tariff barriers between UK and the EU actually impacted the determinants of inward FDI in the UK manufacturing sector. List (2001) examines the influence of pollution regulation on the number of new foreign-acquired firm in California with count models. Tadesse and Ryan (2004), with several count models, look into the host market characteristics and how they affect FDI inflows coming from Japan. Finally, Georgopoulos (2008) uses a negative binomial regression to analyse the role of the exchange rate in outbound Canadian M&A deal in Europe and US.

This study is laid out as follows. The next section describes the main features of the count data models and the limitation of non-count models that make them unsuited to forecast the number of FDI deals in EU. The model finally selected, NB-MIDAS, is presented in Section 3. Section 4 presents the data on the dependent variable and the covariates together with the motivations given by the literature for their use. Finally, results are hosted in Section 5, while Section 6 concludes.

2. Count data and modelling challenges

The special nature of the data, i.e. count data or natural numbers, and the time series structure of the variable we need to forecast (monthly number of deals) heavily conditions the type of models that can be used. We have two choices, either transform count data to fit models developed for continuous data, or use models created for integer-valued data. Furthermore, the use of continuous variables as explanatory variables in a model where the dependent variable is a natural number poses additional constraints.

The first option, i.e. adapting count data through a transformation e.g. a logarithmic function, would allow to use standard estimation procedures but implies several drawbacks, including the assumption on the distribution of the data-generating process which is not supported by count data (**Error! Reference source not found.** contains a summary of this discussions).

The second option, theoretically more grounded, presents the limitation that not all integer-valued models take into account the specific nature of count data (examples are given in Table 1, see also Winkelmann, 2008) and have to be transformed accordingly. We use a negative binomial model where the parameters of the distribution are time-varying based on high-frequency (daily) data. Our model fits the empirical features of the count data, i.e. time-varying overdispersion, while taking into account the daily information useful to improve our monthly forecast, i.e. MIDAS approach. To complement the analysis, the Poisson distribution is used as benchmark.[5]

[Table 1 – Models for non-count data – about here]

The time series of count data used in this paper (i.e. the number of M&A deals) present time-varying overdispersion. Figure 1 shows the daily deals (blue asterisks) grouped by month together with the conditional monthly mean (red line) and the ratio between the conditional variance and the conditional mean, i.e. the so called index of dispersion.[6] We can clearly see the presence of a time varying overdispersion as the aggregated monthly number of inbound EU deals presents a variance 8 times higher than its mean for the period 01/1998-03/2021 (Table 2). Nevertheless, the actual conditional mean is not a fix ratio of the conditional variance (Figure 1), hence the relationship between the conditional mean and the conditional variance is not constant over time and has to be taken into account by modelling the first two moments of the distribution allowing time-varying parameters.

To improve the forecasting performance, we make the assumption that the change in M&A trend for month *t* could be already observed in the last days of the month *t-1*. The idea behind is that investors have a more updated

[5] See Appendix A: "Poisson benchmark for count processes and INGARCH models" where the indices to describe the features of count distributions are defined in terms of the Poisson distribution. In the literature of count-data, the family of Poisson models is often employed for comparison purposes as it plays, for natural numbers, the same role played by the Normal distribution for real-valued continuous data (Weiss, 2017; Winkelmann, 2008). However, some Poisson models either fail to capture features of the real data, such as the overdispersion (Bertrand et al., 2005), or have poor results in diagnostics (Jung et al., 2006; Jung and Tremayne, 2011) or in forecasting (Czado et al., 2009).

[6] To plot the conditional moments (daily mean and variance in month *t*) we have used a rolling window approach with a window length of 12 months.

information set on the state of the economy the closer they are to the moment of the investment. Figure 2 shows the root mean squared percentage error (RMSPE) of the forecast obtained from an OLS regression of the number of deals observed in *t-1* on the number of deals in *t*. The parameter γ is a measure of the importance of the latest deals, for γ=0 all the deals in *t-1* will have the same importance, while for γ>0 the most recent deals will have higher importance for the forecast. It is clear from Figure 2 that a lower RMPSE is associated to γ>1, indicating a higher importance of more recent deals to improve forecasting performance.

[Figure 1 – Aggregate M&A data – about here]

[Table 2 – Descriptive statistics – about here]

[Figure 2 – Forecasting performance of the aggregated M&A data– about here]

3. **The NB-MIDAS approach.**

We propose a negative binomial model where both parameters (η and π) are time-varying. To get a more precise estimation we rely on the two first moments of the distribution. Also, to capture early trends in the future evolution of the count time series we use high frequency data (MIDAS).

The conditional mean is defined as:

$$E(Y_t|\mathcal{F}_{t-1}) = \lambda_t = \alpha\left[\sum_{m=1}^{K} \Psi_m(\omega_1,\omega_2) Y_{t-1}^{(M_{t-1}-m+1)}\right] M_t + \beta\lambda_{t-1} + exp(\boldsymbol{X}_{t-1}\boldsymbol{\gamma}) \qquad (2)$$

where $\boldsymbol{X_{t-1}}$ is a set of exogenous variables known at time t-1, and the exponential transformation ensures the positive values in the conditional mean. M_t is the number of business days of the month we forecast. $Y_{t-1}^{(M_{t-1}-m+1)}$ indicates the observation at day $M_{t-1} - m + 1$ of month t-1, e.g. $Y_{t-1}^{(M_{t-1})}$ is the number of deals in the last day of month t-1, where the subscript indicates the lag month and the superscript indicates the lag day. We employ different lags for the MIDAS structure, in particular, we employ one week, two weeks and one month, i.e. K=5, 10, 21 (we take into account the possibility of having different number of days depending on the month).

$\Psi(\omega_1, \omega_2, m)$ is the function defining the weighting scheme of MIDAS filters. For robustness checks we study the beta weighting function[7] and the exponential Almon weighting function. We use a beta-type polynomial function, as follows:

$$\Psi(\omega_1, \omega_2, m) = \frac{\left(\frac{1-m}{K}\right)^{\omega_1 - 1}\left(\frac{m}{K}\right)^{\omega_2 - 1}}{\sum_{m=1}^{K}\left(\frac{1-m}{K}\right)^{\omega_1 - 1}\left(\frac{m}{K}\right)^{\omega_2 - 1}}, \tag{3}$$

while the exponential weighting function would be defined as:

$$\Psi(\omega_1, \omega_2, m) = \frac{exp(\omega_1 m + \omega_2 m^2)}{\sum_{m=1}^{K} exp(\omega_1 m + \omega_2 m^2)}, \tag{4}$$

The conditional variance is defined as a time-varying ratio of the conditional mean:

$$Var(Y_t|\mathcal{F}_{t-1}) = \lambda_t \kappa_t \tag{5}$$

where $\kappa_t = 1/\pi_t$ and

$$\pi_t = \frac{2}{\left(1 + exp\left(\alpha_0(1-\alpha_1) + (1-\alpha_1)\sum_{j=1}^{T-1}\alpha_1^j\left(\frac{1}{M_{t-j}}\sum_{m=1}^{M_{t-j}}\left(Y_{t-j}^{(M_{t-j}-m+1)} - \frac{\lambda_{t-j}}{M_{t-j}}\right)^2 \Big/ \frac{\lambda_{t-j}}{M_{t-j}}\right)\right)\right)} \tag{6}$$

with $\alpha_1 \in [0,1)$ and $\alpha_0 \geq 0$,

where M_{t-j} is the number of days of the month t-j. λ_{t-j} is the monthly conditional mean of the month corresponding to the lag $Y_{t-j}^{(M_{t-1}-m)}$. It is important to notice that M_{t-j} and μ_{t-j} are constant values for all the days within the same month.

[7] We have also employed the Kumaraswamy function providing similar results to the beta function. Ghysels et al. (2005) indicate several advantages of the beta-type framework. Firstly, the weights are strictly positive and the aggregation of the weights sums to one. Secondly, the MIDAS function can generate, using only parameters ω_1 and ω_2, different shapes of the high-frequency lags, e.g. monotonically increasing, decreasing or humped-shaped.

The model defined in Equations (2) to (6), the negative Binomial MIDAS (henceforth NB-MIDAS), nests the Poisson and the Negative Binomial DIN-type model (Xu et al., 2012). The DIN-type model is obtained with $\alpha_1 = 0$, hence, the $Var(Y_t|F_{t-1}) = E(Y_t|F_{t-1})\frac{2}{1+\exp(\alpha_0)}$ and the parameter π from the NB(η_t, π) would be $\pi = \frac{2}{1+\exp(\alpha_0)}$. The Poisson model can be obtained when the expression within the exponential function in Equation (3) is zero[8], i.e. $\alpha_1 = 0$ and $\alpha_0 = 0$, as $\pi \to 1$. Because $\mathrm{E}(Y_T^m|\ \mathcal{F}_t) = \frac{\lambda_{T|t}}{M_T}$ for $T > t$, the weight of the α_1 section will decrease for long-term forecasts, so we can distinguish between long and short term variance.[9] Indeed Eq. (5) could be decomposed in two parts:

$$Var(Y_t|\mathcal{F}_{t-1}) = \sigma^2_{LR,t} + \sigma^2_{SR,t} \qquad (7)$$

where $\sigma^2_{LR,t} = \frac{\lambda_t(1+exp(\alpha_0(1-\alpha_1)))}{2}$ is the long-run variance and $\sigma^2_{SR,t} = Var(Y_t|\mathcal{F}_{t-1}) - \sigma^2_{LR,t}$ is the short-run variance component.

Our approach introduces three main advantages in the count data fit. Firstly, we rely on the two first moments to estimate the parameters of the model, thereby increasing the robustness of the estimation and allowing for a higher flexibility in the relationship between the conditional mean and variance as compared to DIN-type of models. Secondly, we take advantage of the high frequency data to get a better estimation of the future values of the count process. Finally, we can distinguish between different components in the variance of the count process.

4. Forecast analysis

We estimate the model by means of the Conditional Maximum Likelihood (CML) in order to avoid the forecast bias produced by other methods e.g. those that estimate the parameters of the model minimising the Median Absolute Error (MAE) (Morlidge, 2015).

We study the performance of this innovative model by looking, not only at the point estimates of the forecast, but also at the forecasted distribution of the variable of interest. To compute the forecast performance, we use the Root Mean Squared Forecast Error (RMSFE) and Mean Absolute Percentage Error (MAPE). As the focus should also be set at the correct fit of the entire distribution (Kolassa, 2016), we rely on the Probability Integral Transformation (PIT) and the log predictive score (Czado et al., 2009; Jung and Tremayne, 2011). Finally, we compare the forecast provided by our model with the forecast obtained by standard models for the period 2021Q2-2022Q1.

[8] To get the Poisson distribution we would need that $\pi \to 1$ and $\eta \to \infty$, such that $E(Y_t \mid \mathcal{F}_{t-1}) = \frac{\eta(1-\pi)}{\pi} \to \lambda$

[9] Note that the number of days at month T>t, i.e. M_T, is already known at time t as it is a deterministic value.

4.1. Forecasted distribution

The fit of the entire distribution is represented by a histogram showing the uniform transformation of the data by using the forecast distribution provided by the model. If the data is well fitted, we would observed a box-shape distribution, whereas if we fail to fit the tail of the distribution, we would observe higher bars in low and high quantiles (see for instance Figure 5a).

The relative frequencies are obtained as the ratio between the difference in the forecasted probability integral transformation between two consecutive quantile ranges, and the probability under perfect fit of the data. The more similar is the height of these bar, the better the fit of the forecast values is.

In formula, the figure below shows $\left(\tilde{F}\left(\frac{j}{K}\right) - \tilde{F}\left(\frac{j-1}{K}\right)\right)$ for j=1,2,…,14 where:

$$\tilde{F}(u) = \begin{cases} 0 & u \leq F(k-1|\mathcal{F}_{t-1}) \\ \dfrac{u - F(k-1|\mathcal{F}_{t-1})}{F(k|\mathcal{F}_{t-1}) - F(k-1|\mathcal{F}_{t-1})} & F(k-1|I_{t-1}) \leq u \leq F(k|\mathcal{F}_{t-1}) \\ 1 & u \geq F(k|\mathcal{F}_{t-1}) \end{cases}$$

For > 0 , with $F(\dots)$ being the predictive distribution and

$$\tilde{F}(u) = \begin{cases} \dfrac{u}{F(0|\mathcal{F}_{t-1})} & u \leq F(0|\mathcal{F}_{t-1}) \\ 1 & otherwise \end{cases}$$

For $k = 0$.

Considering the short dataset available, we also include the thresholds within which the null hypothesis of the data coming from a uniform (0,1) distribution is not rejected. These intervals are created similarly to the thresholds for the backtesting exercise in Kupiec (1995). We assume that each observation has 1/K probability of being at each bar, so the distribution of the observations on the PIT histogram would follow a Bin(T,1/K), where T indicates the number of out-of-sample observations. We build a likelihood ratio as follows:

$$\Lambda(x) = \frac{p^x(1-p)^{T-x}}{\left(\frac{T-x}{T}\right)^{T-x}\left(\frac{x}{T}\right)^x}$$

where $-2\log(\Lambda) \sim \mathrm{X}_1$ under the null hypothesis (Lehmann & Romano, 2006). This technique allows us to check whether the data structure is fitted correctly in short sample time series. To our knowledge, this is the first study in count models that uses a statistic criterion for small samples in the PIT histogram.

We also employ a numerical score based on the predictive distribution of the future number of deals actually observed. We use the log predictive score (LPS) to evaluate this forecast, defined as

$LPS = \sum_t \log(P(Y = y_t | \mathcal{F}_{t-1}),$

Where the highest is the LPS value the better forecast distribution is fitted by the model.

4.2. Forecast performance

We compute the Mean Absolute Percentage Error (MAPE) for the out-of-sample period. The median forecast of the number of M&A deals minimizes the MAPE and, hence, it is the main measure to check the forecasting properties (Hanley et al., 2001).The Mean Absolute Percentage Error (MAPE) is defined as follows:

$$MAPE = \frac{1}{T-k} \frac{\sum_{t=k}^{T} |y_t - \tilde{y}_{t|t-1}|}{y_t}, \quad (5.2.2)$$

where $\tilde{y}_{t|t-1}$ is such that $P(Y_t < \tilde{y}_{t|t-1}) = 0.5$ and the subscript $t|t-1$ indicates that the forecast is computed with the information up to t-1. The scale feature of the MAPE measure, i.e. the outcome does not depend on the number of deals, is a main advantage against the mean absolute error (MAE).

We also compute as a robustness measure the Root Mean Squared Forecast Error (RMSFE), which is defined as,

$$RMSFE = \frac{1}{T-k} \sqrt{\sum_{t=k}^{T} (y_t - \mathrm{E}(y_t|\mathcal{F}_{t-1}))^2}, \quad (5.2.3)$$

where the focus is in the mean forecast instead of the median forecast as the MAPE measure.

5. Data

The variable to be forecasted in this study is the monthly number of inbound M&A in the European Union (EU[10]), i.e. the number of M&A transactions with investors located outside the EU. The data sample begins in 1998 and

[10] EU is intended as EU27.

ends in the first quarter of 2021. The M&A information is retrieved from the Bureau van Dijk's Zephyr database, which has a better disclosure of information, especially for multideals, than other data sources.[11] Each M&A deal is associated to the month in which the announcement is made, which according to the Zephyr, corresponds to the date *"when details of the deal have been provided, when a formal offer has been made or when one of the companies involved in the deal has confirmed that the deal is to go ahead".* Identifying the deal at this stage, allows us to analyse the desire to merge, which could be different to the actual mergers due to, for instance, the intervention of the regulatory scrutiny.[12] Concerning the size of the deals in our sample, we consider those deals in which the final stake acquired by the investor is at least 10% of the target company. We use the interval from 01/08/2009 to 31/03/2021 (139 observations) as the out-of-sample period to analyse and compare the properties of the different models for the one-month ahead forecast of the inbound EU deals.

Figure 3 provides the histogram of the monthly number of aggregated inbound M&A deals, showing a right skewness and unimodal distribution around a sample average of 120 deals.

[Figure 3 – Histogram of the aggregated M&A deals – about here]

The forecast exercise, in addition to the aggregate approach discussed above, will also be repeated distinguishing: (1) the region of origin of the foreign investor, (2) the target sector and (3) the technological intensity of the target sector. Regarding the region of origin of the foreign investor we identify 6 regions that correspond to more than 90% inbound deals in the EU for the sample period. These regions are: a) United States and Canada, b) United Kingdom, c) EFTA region (Iceland, Norway and Switzerland), d) Offshore countries, e) Developed Asian region (Japan, Singapore, Taiwan and South Korea) and f) China. The literature has pointed out the market size (Billington, 1999; Culem, 1988; Dunning, 1980; Sader, 1993; Shamsuddin, 1994; Tsai, 1994) and macroeconomic stability (Boateng et al., 2014; Coskun, 2001) as the main determinants of regional M&A deals. Consequently, we employ the one-quarter lag of annual growth of the GDP of the EU, the GDP growth from the foreign investor region[13] and the World Uncertainty Index for Europe[14] as indicators of macroeconomic conditions. Data are obtained from Eurostat and the

[11] See for instance Bollaert & Delanghe (2015).
[12] According to the information available in Zephyr regarding the completed and assumed completed deals over the total number of announced deals, most of the announced deals are completed. The current pandemic situation, however, has produced an increase of the pending deals (OECD, 2020a).
[13] For the aggregated M&A deals, we use the GDP growth of OECD countries (excluding EU). No foreign GDP growth variable is employed in the offshore case.
[14] https://fred.stlouisfed.org/series/wuieurope.

Federal Reserve of St. Louis. Forecast for the period 2021 is provided by the ECOFIN forecast and, when the forecast is not available, we compute an AR(4) to obtain the future evolution of the covariates.

[Figure 4 – Decomposition of the aggregated M&A data by region of origin– about here]

Concerning the inbound M&A deals by sector of the target company, three main sectors are studied: a) Manufacturing, b) Services, and c) Banking and Insurance.[15] We employ as exogenous variables the growth of value added and productivity of the target sector compared to the same quarter of the previous year. The data is retrieved from the ECB SDW. Forecasted evolution for the covariates is obtained from the AR(4) model.

Finally, we also decompose the deals with targets in the manufacturing sector according to the degree of Hi-tech content of the target sectors' activity, distinguishing between high and medium-high technological intensity, and low and medium-low technological intensity.[16] We employ as covariates the growth of the volume index of production for the high-technology (low-technology) manufacturing sector. The data is retrieved from Eurostat and the forecast for the period 2021 is computed from an AR(4) model to get the future evolution of the covariates.

6. Results

The results are displayed in figures 5 to 12. Odd figures present in the top charts forecasted distribution indicators, i.e. PIT and log-predictive score, whereas bottom charts present some measure of forecast performance, i.e. RMSFE and MAPE. Even figures provide the one-year ahead forecast for the different count series, where we compare the forecast according to different models.

6.1. Aggregate EU inbound deals

Figure 5 provides in the top charts the Probability Integral Transformation and the log predictive score for the aggregate EU inbound deals, showing that the NB-MIDAS presents the best results. On the one hand, according to the PIT graph and the bounds at 99%, we cannot reject the hypothesis that the probability integral transformation

[15] Sectors are classified using the NACE Rev. 2, 2-digit. Specifically, Manufacturing includes codes ranging from 10 to 33 and from 41 to 43, Services from 45 to 63 and from 68 to 75, and Banking and Insurance from 64 to 66.
[16] We follow the aggregation of manufacturing based on NACE Rev. 2. High and medium-high manufacturing industries includes codes 20, 21, 26 and from 27 to 30. Low and medium-low manufacturing industries includes codes from 10 to 19, 22 to 25 and 31 to 33.

obtained from the NB-MIDAS is distributed uniformly, whereas for the INGARCH models we reject this null hypothesis. Similarly, we obtain the highest log-predictive scores using the NB-MIDAS, showing that the overall forecasted distribution is better fitted under our proposed model. Bottom charts from figure 5 also indicate that our model provides the best point forecast performance, both in terms of mean (RMSFE) and median (MAPE).

[Figure 5 – Forecasted distribution and forecast performance of the aggregated M&A deals – about here]

Figure 6 presents in the left chart the one-year ahead forecast of our model compared to the forecast provided by the INGARCH models. This chart shows a similar behaviour of the median of our model as compared to other models but a different evolution of the 90% confidence interval represented by the blue area. Indeed, for long horizons, our model discards the short term behaviour, which is the results of the high-frequency data, providing narrower confidence intervals as the short-run variance component fades away. The right graph of the same figure indicates the evolution of the one-month ahead forecasted variance, which shows that the long-run component of the one-month ahead variance is close to the Poisson-INGARCH variance, whereas the variance under the NB-MIDAS is around the variance provided by the NB-INGARCH, showing that our model presents a higher degree of flexibility to capture swifts in the variance of the count process.

[Figure 6 – One-year ahead forecast and one-month ahead out-of-sample variance for the aggregated M&A deals – about here]

6.2. Results by origin of the Investor

The investors are grouped in 6 regions/countries (Figure 7): United States (US) and Canada, United Kingdom (UK), EFTA (Switzerland, Norway and Iceland), Offshore countries (OFC)[17], Developed Asia (Japan, Singapore, Taiwan and South Korea), and China.

[17] Offshore financial centres are defined according to IMF (2014) "Offshore Financial Centers (OFCs): IMF Staff Assessments" (available at http://www.imf.org/external/NP/ofca/OFCA.aspx) and IMF (2000) "Offshore Financial Centres" IMF Background Paper (available at http://www.imf.org/external/np/mae/oshore/2000/eng/back.htm#table1). The main Offshores by number of deals or greenfields are (alphabetical order) Bermuda, British Virgins Islands, Cayman Islands, Mauritius and the UK Channel islands.

Panel A focuses in the US and Canada region, with the top charts displaying the Probability Integral Transformation and the log predictive score. According to the PIT graph and the bounds at 99%, we cannot reject that the probability integral transformation obtained from the NB-MIDAS or NB-INGARCH is distributed uniformly, whereas for the Poisson INGARCH model we do reject this null hypothesis. Actually, the fit of the Poisson is much worse in lower and higher quantiles, pointing to the limitation of Poisson models to capture over and under dispersion. Similarly, the log-predictive score provides the worst results with the Poisson INGARCH model. Bottom charts from Panel A also indicate that our model provides the best point forecast performance in terms of median (MAPE), whereas the NB-INGARCH provides better results in terms of mean (RMSFE). The good performance of NB-MIDAS relies on the extra information brought by high-frequency data, hence, the less informative is the high-frequency data and the lower will be the additional advantages conveyed to the model. In particular, for count processes with a low number of counts (e.g. M&A deals in EU from countries such as Turkmenistan), the high-frequency data is not likely to provide relevant additional information, as more zeros will be observed.

United Kingdom is displayed in Panel B. According to the PIT graph and the bounds at 99%, we cannot reject the null hypothesis of uniform distribution for the probability integral transformation obtained from the NB-MIDAS or NB-INGARCH, instead for the Poisson INGARCH model we reject this null hypothesis. Similarly, the log-predictive score provides the worst results under the Poisson INGARCH model. Bottom charts from Panel B also indicate that our model provides the best point forecast performance in terms of median (MAPE), whereas the NB-INGARCH provides better results in terms of mean (RMSFE).

Panel C focuses on the EFTA region where we cannot reject that the probability integral transformation obtained from the NB-MIDAS or NB-INGARCH is distributed uniformly. Again, for the Poisson INGARCH model we reject this null hypothesis. Similarly to UK, the log-predictive score provides the worst results under the Poisson INGARCH model, while NB-MIDAS supplies the best point forecast performance in terms of median (MAPE). The NB-INGARCH provides better results in terms of mean (RMSFE).

For OFC countries (Panel D) the uniform distribution for the probability integral transformation obtained from the NB-MIDAS or NB-INGARCH cannot be rejected, while this null is rejected for the Poisson INGARCH model. The log-predictive score provides the worst results under the Poisson INGARCH model while the NB-MIDAS shows the best results. Bottom charts from Panel D also indicate that our model provides the best point forecast performance in terms of mean (RMSFE), whereas the NB-INGARCH provides better results in terms of median (MAPE).

Panels E and F focus on the Developed Asia region and China, respectively. According to the PIT graph on the top figure, we can reject at 99% confidence level the uniformly distribution of the PIT for China under the INGARCH models, whereas this rejection is constraint for the Poisson INGARCH model for Developed Asian region. Similarly, for both regions, the log-predictive score provides the worst results under the Poisson INGARCH model providing the NB-MIDAS the best results. Bottom charts from these panels indicate that our model provides the best point forecast performance in terms of mean (RMSFE), while the NB-MIDAS also provides better results in terms of the median (MAPE) for China.

[Figure 7 – Forecasted distribution and forecast performance of the M&A deals by region of the acquirer – about here]

The one-year head forecast presented in Figure 8 shows a slightly increase of the M&A deals coming from US and Canada, China and EFTA region, a decrease of those coming from the OFCs and a sharp increase of deals from Developed Asia that reaches the pre-Covid level.

[Figure 8 – One-year ahead forecast for the M&A deals by region of the acquirer – about here]

6.3. Results by sector of the target company

Figure 9 provides 3 panels of charts, one for each sector analysed (manufacturing, services, banking). For all three sectors we cannot reject the null of uniform distribution for the probability integral transformation obtained from the NB-MIDAS. Instead, for the Poison INGARCH model we always reject this null hypothesis.

For all the sectors the log-predictive score provides the worst results under the Poisson INGARCH model providing the NB-MIDAS the best results (second best in case of Services). Our model provides the best point forecast performance both in terms of mean (RMSFE) and median (MAPE) for manufacturing. While for services the top score in terms of mean (RMSFE) goes to the NB-INGARCH. For banking the reverse happens, our model has the top score for the mean while NB-INGARCH provides better results in terms of median (MAPE).

[Figure 9 – Forecasted distribution and forecast performance of the M&A deals by sector of the target – about here]

Regarding the one-year ahead forecast shown by Figure 10, all the models tested forecast an increased number of M&A in the manufacturing and service sector, although our model is slightly more pessimistic. Forecasts in the banking sector indicate, instead, no significant changes in the number of deals for the next year.

[Figure 10– One-year ahead forecast for the M&A deals by sector of the target – about here]

6.4. Results by according to the technological intensity of the target company in the manufacturing sector

Figure 11 provides 2 panels of charts, one for each type of manufacturing sector analysed. For both high and medium-high technology manufacturing sector and for low and medium-low technology manufacturing sector we cannot reject that the probability integral transformation obtained from the NB-MIDAS or NB-INGARCH is distributed uniformly, whereas for the Poisson INGARCH model we reject this null hypothesis. Similarly, the log-predictive score provides the worst results under the Poisson INGARCH model providing the NB-MIDAS the best results. Bottom charts from Panels A and B also indicate that our model provides the best point forecast performance in terms of mean (RMSFE) and median (MAPE) for all technological intensities. Regarding the one-year ahead forecast shown by Figure 12, all the models forecast an increase in the number of inbound M&As in EU.

[Figure 11 – Forecasted distribution and forecast performance of the M&A deals by tech-intensity of the target – about here]

[Figure 12– One-year ahead forecast for the M&A deals by tech-intensity of the target – about here]

7. Conclusions

The practical organisation of the FDI screening in public administrations calls for a thorough forecast of the number of deals that will lead to notification, permitting the efficient organisation of the screening activity. Additionally, Coronavirus crisis has put strategic sectors in a vulnerable position, leading to the exposure of European firms to foreign investors' acquisitions. Consequently, forecasting M&A deals becomes crucial as an early-warning measure

of FDI trend changes. We propose a new model that enriches the benchmark INGARCH. Our NB-MIDAS uses high-frequency (daily) data to improve the forecasting properties of the INGARCH. By relying on the first two moment of the distribution we are able to obtain both a time-varying mean and overdispersion parameter of the count process. Additionally, the NB-MIDAS enable us to decompose the variance singling out short-term and long-term variance components. This is especially interesting as it allows take into account short-term dynamics which would be faded out in the long terms and would explain the variation of the overdispersion parameter, linking the DIN-INGARCH models to the NB-INGARCH models.

We analyse the forecasted distribution and the point forecasts of our model in comparison with benchmark models to forecast inbound M&A deals in EU at aggregate, regional and sectorial levels. Results suggest that our model improve the previous approaches on different dimensions, especially in terms of the overall forecasted distribution but also in the point estimate forecast.

The forecast exercise shows that at the aggregate level we expect an increase up to 8% in the number of foreign acquisitions in the next quarter following March 2021, yet lagging behind compared to the pre-crisis levels. The actual increase was close to 11%. Forecasts distinguishing across investors' origin country show that an upward trend is expected mainly for Developed Asia investors, while more modest increase is associated to US and Canada, China and EFTA region, with OFC lagging behind in the coming months. Finally forecasted deals are on the rise mainly for manufacturing and services with no difference for high and low-tech manufacturing sectors.

References

Agosto, A., & Ahelegbey, D. F. (2020). Default count-based network models for credit contagion. *Journal of the Operational Research Society*, *0*(0), 1–14. https://doi.org/10.1080/01605682.2020.1776169

Agosto, A., Cavaliere, G., Kristensen, D., & Rahbek, A. (2016). Modeling corporate defaults: Poisson autoregressions with exogenous covariates (PARX). *Journal of Empirical Finance*, *38*, 640–663. https://doi.org/10.1016/j.jempfin.2016.02.007

Agosto, A., & Giudici, P. (2020). A poisson autoregressive model to understand covid-19 contagion dynamics. *Risks*, *8*(3), 1–8. https://doi.org/10.3390/risks8030077

Bertrand, O., Mucchielli, J.-L., & Zitouna, H. (2005). Location Choices of Multinational Firms: The Case of Mergers and Acquisitions. *SSRN Electronic Journal*, *22*(1), 181–209. https://doi.org/10.2139/ssrn.556206

Billington, N. (1999). The location of foreign direct investment: an empirical analysis. *Applied Economics*, *31*(1), 65–76. https://doi.org/10.1080/00036846.2019.12067087

Boateng, A., Hua, X., Uddin, M., & Du, M. (2014). Home country macroeconomic factors on outward cross-border mergers and acquisitions: Evidence from the UK. *Research in International Business and Finance*, *30*(1), 202–216. https://doi.org/10.1016/j.ribaf.2013.08.001

Bollaert, H., & Delanghe, M. (2015). Securities Data Company and Zephyr, data sources for M&A research. *Journal of Corporate Finance*, *33*, 85–100. https://doi.org/10.1016/j.jcorpfin.2015.05.005

Coskun, R. (2001). Determinants of direct foreign investment in Turkey. *European Business Review*, *13*(4), 221–227. https://doi.org/10.1108/EUM0000000005536

Culem, C. G. (1988). The locational determinants of direct investments among industrialized countries. *European Economic Review*, *32*(4), 885–904. https://doi.org/10.1016/0014-2921(88)90051-7

Czado, C., Gneiting, T., & Held, L. (2009). Predictive model assessment for count data. *Biometrics*, *65*(4), 1254–1261. https://doi.org/10.1111/j.1541-0420.2009.01191.x

Dunning, J. H. (1980). Theory Toward an Eclectic Production : of International Tests Some Empirical. *Journal of International Business Studies*, *11*, 9–31. http://www.jstor.org/stable/154142

Ferland, R., Latour, A., & Oraichi, D. (2006). Integer-valued GARCH process. *Journal of Time Series Analysis*, *27*(6), 923–942. https://doi.org/10.1111/j.1467-9892.2006.00496.x

Fokianos, K. (2011). Some recent progress in count time series. *Statistics*, *45*(1), 49–58. https://doi.org/10.1080/02331888.2010.541250

Fokianos, K., Rahbek, A., & Tjøstheim, D. (2009). Poisson autoregression. *Journal of the American Statistical Association*, *104*(488), 1430–1439. https://doi.org/10.1198/jasa.2009.tm08270

Georgopoulos, G. J. (2008). Cross-border mergers and acquisitions: Does the exchange rate matter? Some evidence for Canada. *Canadian Journal of Economics*, *41*(2), 450–474. https://doi.org/10.1111/j.1365-2966.2008.00470.x

Ghysels, E., Santa-Clara, P., & Valkanov, R. (2005). There is a risk-return trade-off after all. *Journal of Financial Economics*, *76*(3), 509–548. https://doi.org/10.1016/j.jfineco.2004.03.008

Girma, S. (2002). The process of European integration and the determinants of entry by non-EU multinationals in UK manufacturing. *Manchester School*, *70*(3), 315–335. https://doi.org/10.1111/1467-9957.00305

Hanley, J. A., Joseph, L., Platt, R. W., Chung, M. K., & Belisle, P. (2001). Visualizing the Median as the Minimum-Deviation Location. *The American Statistician*, *55*, 150–152. https://econpapers.repec.org/RePEc:bes:amstat:v:55:y:2001:m:may:p:150-152

Heinen, A. (2011a). Modelling Time Series Count Data: An Autoregressive Conditional Poisson Model. *SSRN Electronic Journal*, 1–38. https://doi.org/10.2139/ssrn.1117187

Heinen, A. (2011b). Modelling Time Series Count Data: An Autoregressive Conditional Poisson Model. *SSRN Electronic Journal*. https://doi.org/10.2139/ssrn.1117187

Hijzen, A., Görgand, H., & Manchin, M. (2008). Cross-border mergers and acquisitions and the role of trade costs. *European Economic Review*, *52*(5), 849–866.

Jung, R. C., Kukuk, M., & Liesenfeld, R. (2006). Time series of count data: modeling, estimation and diagnostics. *Computational Statistics and Data Analysis*, *51*(4), 2350–2364. https://doi.org/10.1016/j.csda.2006.08.001

Jung, R. C., & Tremayne, A. R. (2011). Useful models for time series of counts or simply wrong ones? *AStA Advances in Statistical Analysis*, *95*(1), 59–91. https://doi.org/10.1007/s10182-010-0139-9

Kolassa, S. (2016). Evaluating predictive count data distributions in retail sales forecasting. *International Journal of Forecasting*, *32*(3), 788–803. https://doi.org/10.1016/j.ijforecast.2015.12.004

Kupiec, P. (1995). Techniques for verifying the accuracy of risk measurement models. *The J. of Derivatives*, *3*(2).

Lehmann, E. L., & Romano, J. P. (2006). *Testing statistical hypotheses*. Springer Science & Business Media.

List, J. A. (2001). US county-level determinants of inbound FDI: Evidence from a two-step modified count data model. *International Journal of Industrial Organization*, *19*(6), 953–973. https://doi.org/10.1016/S0167-7187(99)00051-X

Morlidge, S. (2015). Measuring the Quality of Intermittent-Demand Forecasts: ItÕs Worse than WeÕve Thought! *Foresight: The International Journal of Applied Forecasting*, *37*, 37–42. https://econpapers.repec.org/RePEc:for:ijafaa:y:2015:i:37:p:37-42

OECD. (2020a). Foreign direct investment flows in the time of COVID-19. In *OECD* (Issue May). https://www.oecd.org/coronavirus/policy-responses/foreign-direct-investment-flows-in-the-time-of-covid-19-a2fa20c4/

OECD. (2020b). Investment Policy Responses to Covid -19. In *OECD* (Issue June). http://www.oecd.org/coronavirus/policy-responses/oecd-investment-policy-responses-to-covid-19-4be0254d/

Pozzolo, D., & Focarelli, A. F. (2008). Cross-border M&As in the financial sector: Is banking different from insurance?. *Journal of Banking & Finance*, *32*(1), 15–29.

Sader, F. (1993). Privatization and Foreign Investment in the Developing World, 1988-92. *Policy Research Working Papers- World Bank Wps*, ALL.

Shamsuddin, A. F. M. (1994). Economic Determinants of Foreign Direct Investment in Less Developed Countries. *The Pakistan Development Review*, *33*(1), 41–51. http://www.jstor.org/stable/41259744

Tadesse, B., & Ryan, M. (2004). Host market characteristics, FDI and the FDI - Trade relationship. *Journal of*

International Trade and Economic Development, *13*(2), 199–229. https://doi.org/10.1080/0963819042000218683

Tsai, P. (1994). Determinants of foreign direct investment and its impact on economic growth. *Journal of Economic Development*, *19*(1), 138–163.

Weiss, C. H. (2017). An introduction to discrete-valued time series. In *An Introduction to Discrete-Valued Time Series*. https://doi.org/10.1002/9781119097013

Weiß, C. H. (2009). Modelling time series of counts with overdispersion. *Statistical Methods and Applications*, *18*(4), 507–519. https://doi.org/10.1007/s10260-008-0108-6

Winkelmann, R. (2008). Econometric analysis of count data. In *Econometric Analysis of Count Data*. https://doi.org/10.1007/978-3-540-78389-3

Xu, H. Y., Xie, M., Goh, T. N., & Fu, X. (2012). A model for integer-valued time series with conditional overdispersion. *Computational Statistics and Data Analysis*, *56*(12), 4229–4242. https://doi.org/10.1016/j.csda.2012.04.011

Zhu, F. (2012). Modeling overdispersed or underdispersed count data with generalized Poisson integer-valued GARCH models. *Journal of Mathematical Analysis and Applications*, *389*(1), 58–71. https://doi.org/10.1016/j.jmaa.2011.11.042

Tables and Figures

Table 1: Models for non-count data adapted for count data and their limitations

Model	Advantages	Disadvantages
Normal linear regression $y = x\beta + \epsilon$ $\epsilon \sim N(0, \sigma^2)$	Normal distribution approximates the Poisson distribution if the mean is higher than 20.	No possible inference on single outcomes, i.e. P(X=x) is close to zero in continuous distributions. The model allows for a negative outcome. The prediction is not coherent, i.e. the forecast is not an integer-valued outcome.
Log-Linear model $\log(y) = x\beta + \epsilon$ $\epsilon \sim N(0, \sigma^2)$	The variable y is modelled as a log-normal variable.	The zeros in the data have to be deleted to estimate this model. This leads to endogenous sample selection problems. The prediction is not coherent, i.e. the forecast is not an integer-valued outcome. There is a restriction on the conditional variance, i.e. it must be quadratic in the conditional expectation.[18]
Log-linear model with constant c to deal with zeros $\log(y + c) = x\beta + \epsilon$	The model can be estimated even if there are zero in the dataset.	The log(y) is not linear in x, which introduces a bias in the estimation of the model.

[18] If a variable y follows a log-normal distribution, the following identity holds $Var(y|x) = \left(e^{\sigma^2} - 1\right)[E(y|x)]^2$.

$\epsilon \mid x \sim N(0, \sigma^2)$		The prediction is not coherent, i.e. the forecast is not an integer-valued outcome.
Non-linear model $y = \exp(\mathrm{x}\beta) + \epsilon$ $\epsilon \sim N(0, \sigma^2)$	There is no problem in dealing with zero values.	The model allows for a negative outcome. The prediction is not coherent, i.e. the forecast is not an integer-valued outcome.
Ordered Probit and Logit State equation: $y^* = x\beta + \epsilon$ Observation equation: $y = 0 \; if \; y^* < \alpha_0$ $y = 1 \; if \; \alpha_0 \leq y^* < \alpha_1$ $y = 2 \; if \; \alpha_1 \leq y^* < \alpha_2$ $\vdots$	They take into account the integer-valued structure of the data. The prediction can be coherent, i.e. if we wanted to forecast the future median value, it would be a integer-valued outcome.	They do not reflect the underlying count process. The forecast is limited to values already observed in the data. Excessive complexity when the number of counts is high.

Source: (Winkelmann, 2008)

Table 2: Descriptive statistics

	Total	United States and Canada	United Kingdom	Offshore countries	EFTA region	Developed Asian region	China
Mean	126.53	45.29	29.43	17.37	6.85	8.90	5.11
Standard deviation	33.26	12.67	9.40	6.30	4.58	4.53	4.56
Excess skewness	0.19	-0.01	0.33	0.37	2.37	0.51	0.89
Excess kurtosis	-0.27	0.27	0.41	0.32	16.76	1.03	1.74
Index of dispersion	8.74	3.55	3.00	2.28	3.06	2.31	4.07
Zero index	1.00	1.00	1.00	1.00	1.00	1.00	1.02

Note: Excess skewness and kurtosis is defined as the difference with respect to the Poisson distribution. The definition of the index of dispersion and zero index is provided in the section "Poisson benchmark for count processes and INGARCH models".

Figure 1: Daily data of the inbound EU deals and its conditional monthly mean and ratio between conditional mean and variance.

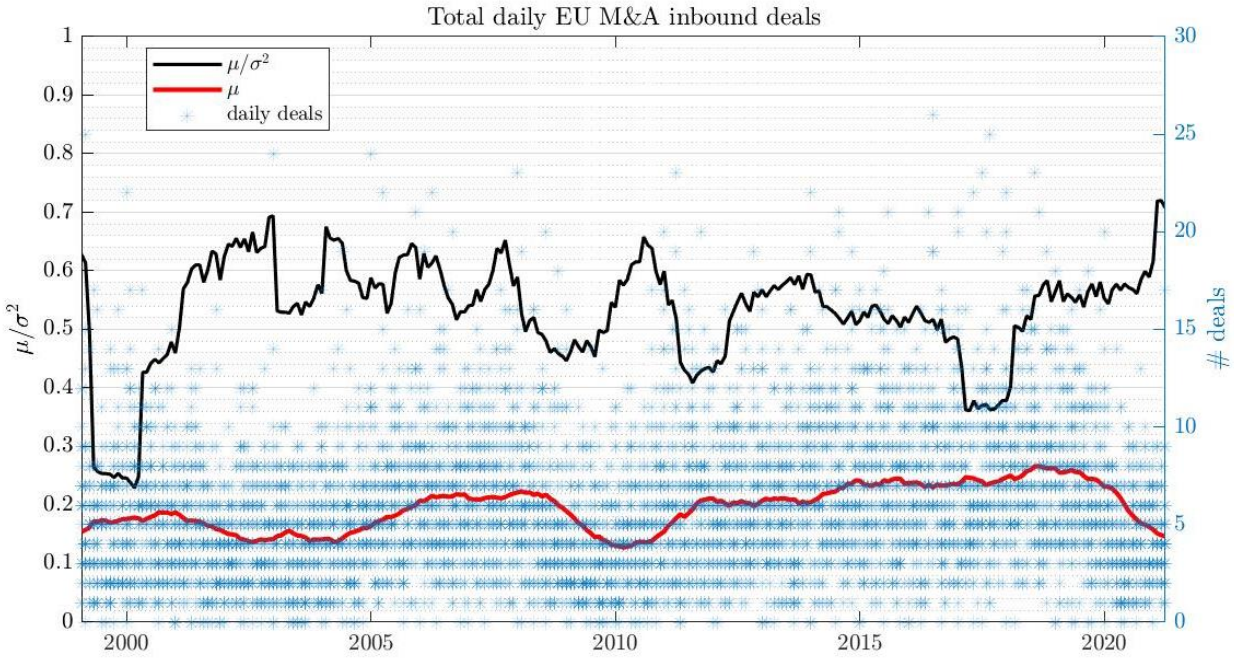

Figure 2: Forecast performance in terms of RMSPE and the weighted average of the past data.

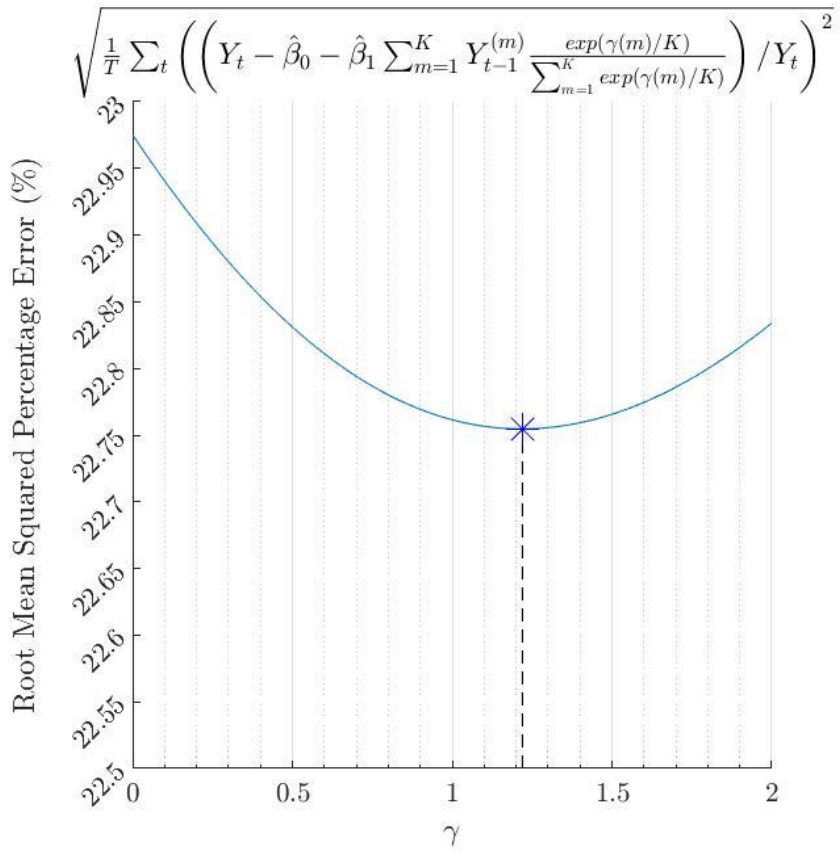

Figure 3: Histogram of the aggregated M&A deals.

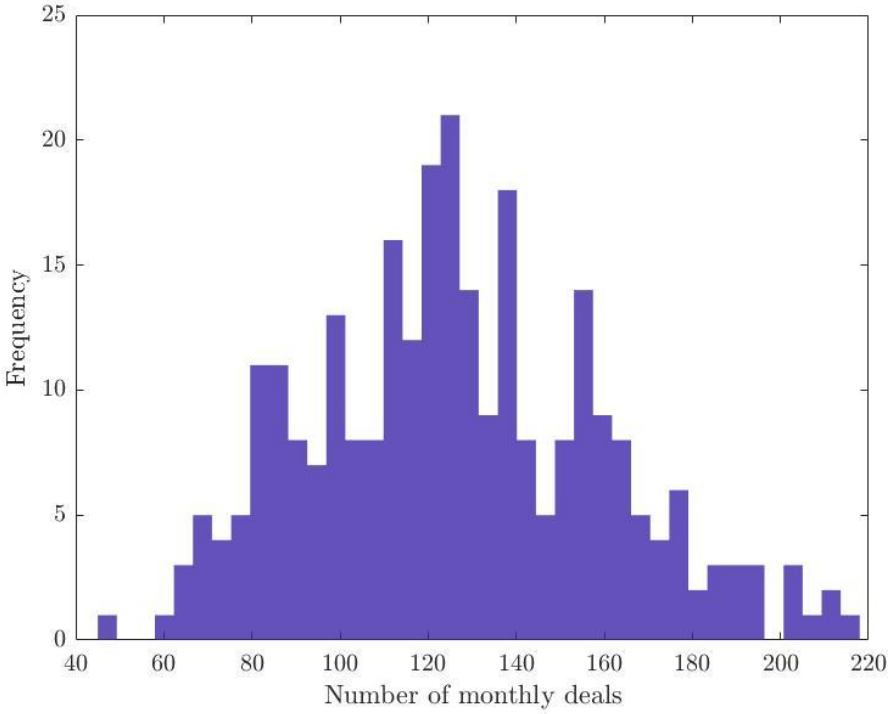

Figure 4: Decomposition of the aggregated M&A deals by the main regions of origin

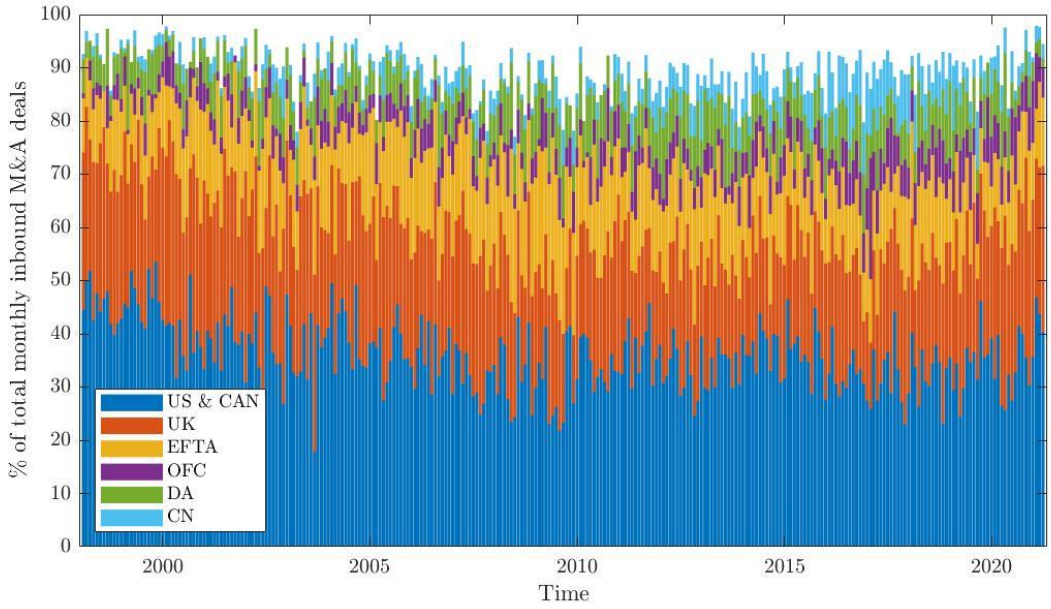

Note: US & CAN: United States and Canada; UK: United Kingdom; EFTA: Iceland, Liechtenstein, Norway and Switzerland; OFC: Offshore Financial Centres; DA: Developed Asia (Japan, Singapore, Taiwan and South Korea); CN: China.

Figure 5: Forecasted distribution and forecast performance for the aggregated M&A deals

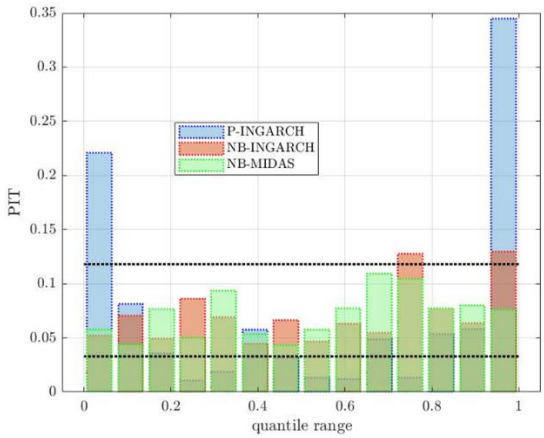

a) Probability Integral Transformation (PIT)

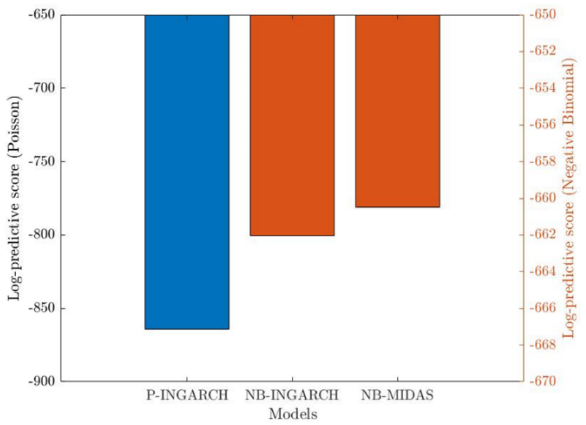

b) Log predictive score

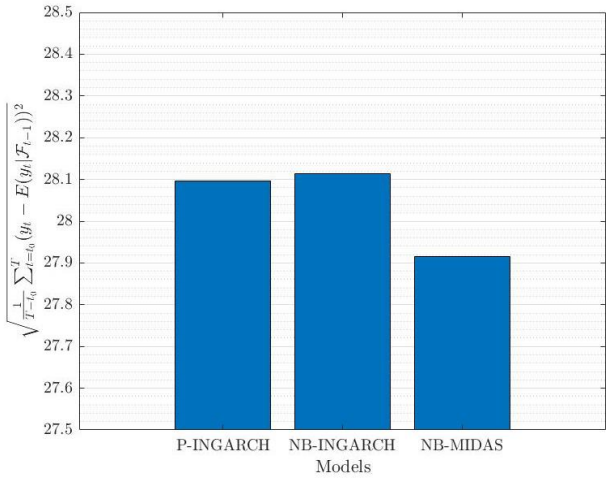

c) Root Mean Squared Forecast Error (RMSFE)

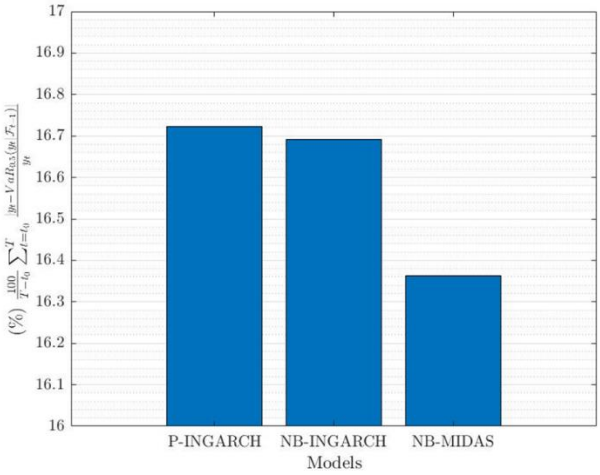

d) Mean Absolute Percentage Error (MAPE)

Note: Top figures gather different measures to analyse the forecasted distribution. Top left figure provides the PIT chart, whereas top right shows the log predictive score. Bottom figures focuses in the point estimates of the forecast, looking at the mean (RMSFE) and median (MAPE).

Figure 6: Forecast for the M&A deals for the period 03/2021-03/2022 and its one-month ahead variance for the out-of-sample period.

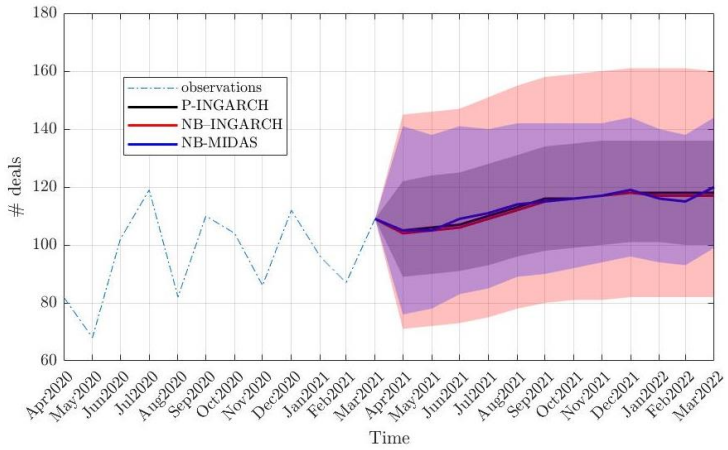

a) Out-of-sample forecast for the period 03/2021-03/2022

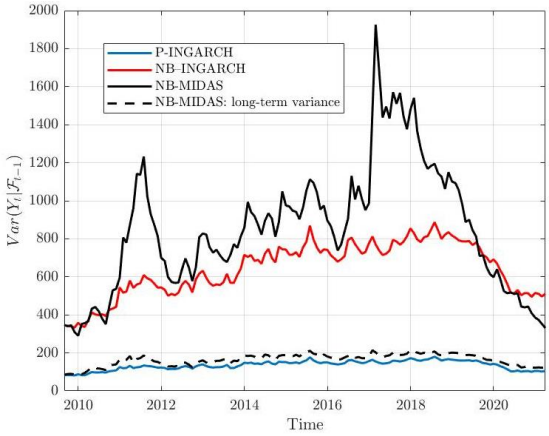

b) One-month ahead out-of-sample forecast variance.

Note: Left figure shows the out-of-sample forecast median under different models together with the 90% confidence interval. Right figure presents the one-month ahead forecast for the variance under the different models.

Figure 7: Forecasted distribution and forecast performance for the regional inbound European M&A deals.

Panel A. US and Canada

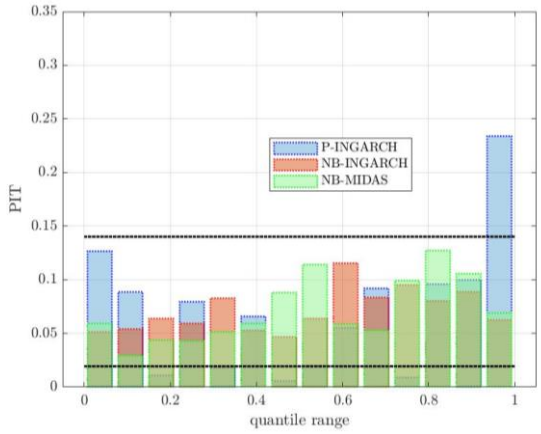

a) Probability Integral Transformation (PIT)

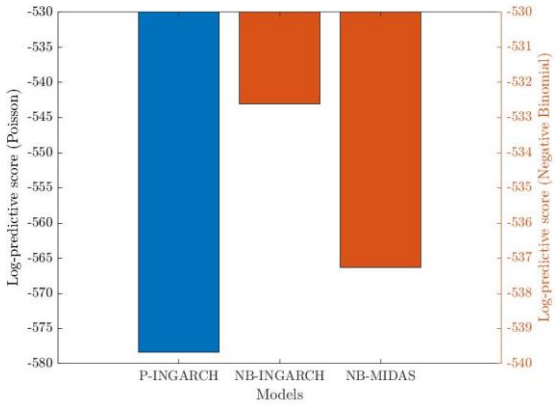

b) Log predictive score

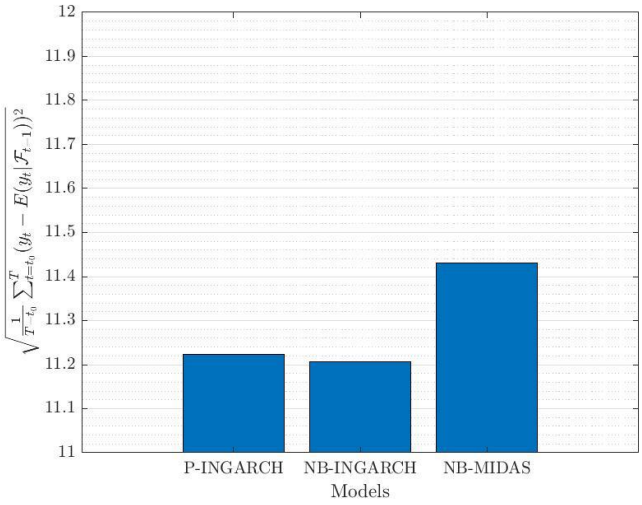

c) Root Mean Squared Forecast Error (RMSFE)

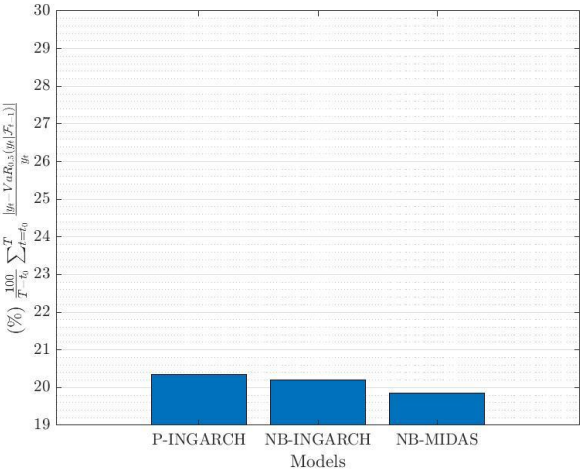

d) Mean Absolute Percentage Error (MAPE)

Note: Top figures gather different measures to analyse the forecasted distribution. Top left figure provides the PIT chart, whereas top right shows the log predictive score. Bottom figures focuses in the point estimates of the forecast, looking at the mean (RMSFE) and median (MAPE).

Panel B. United Kingdom

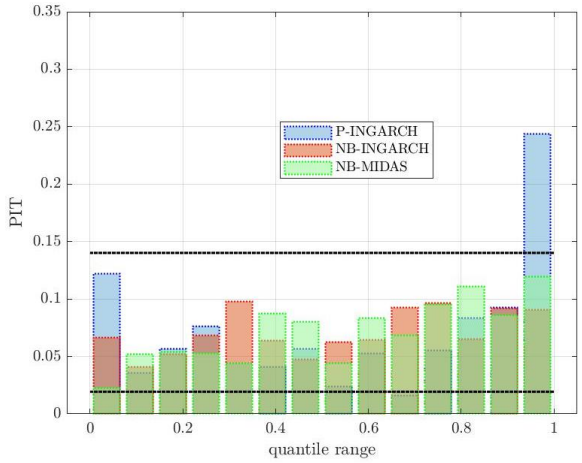

a) Probability Integral Transformation (PIT)

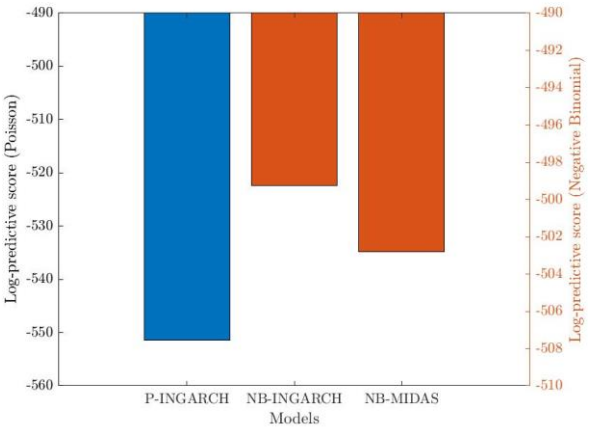

b) Log predictive score

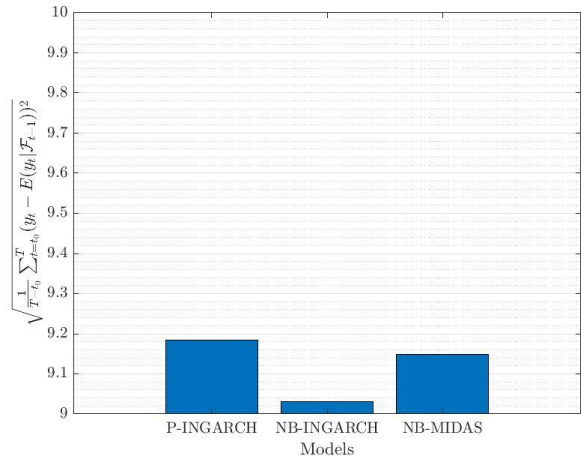

c) Root Mean Squared Forecast Error (RMSFE)

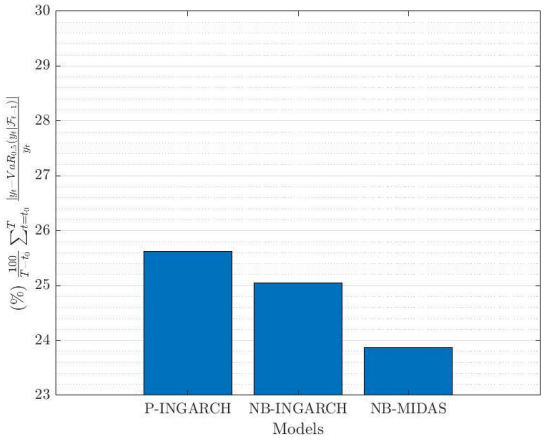

d) Mean Absolute Percentage Error (MAPE)

Note: Top figures gather different measures to analyse the forecasted distribution. Top left figure provides the PIT chart, whereas top right shows the log predictive score. Bottom figures focuses in the point estimates of the forecast, looking at the mean (RMSFE) and median (MAPE).

Panel C. EFTA

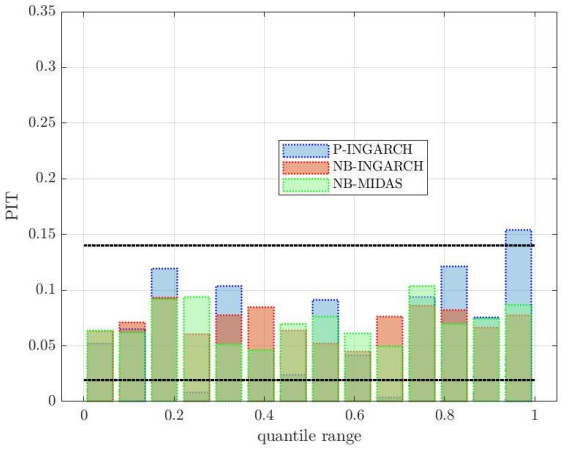

a) Probability Integral Transformation (PIT)

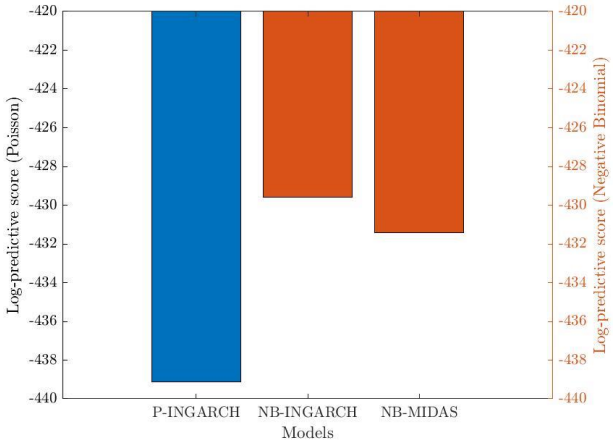

b) Log predictive score

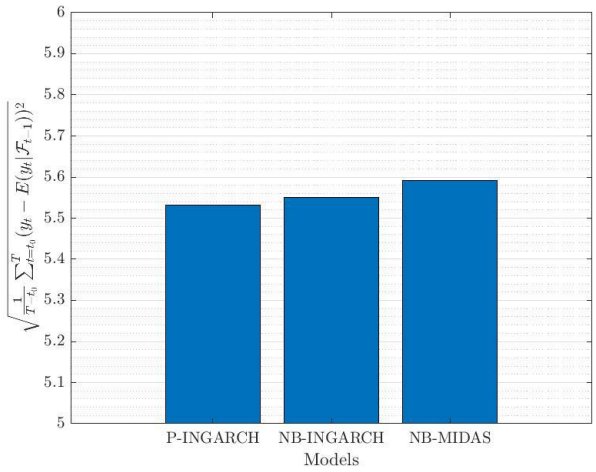

c) Root Mean Squared Forecast Error (RMSFE)

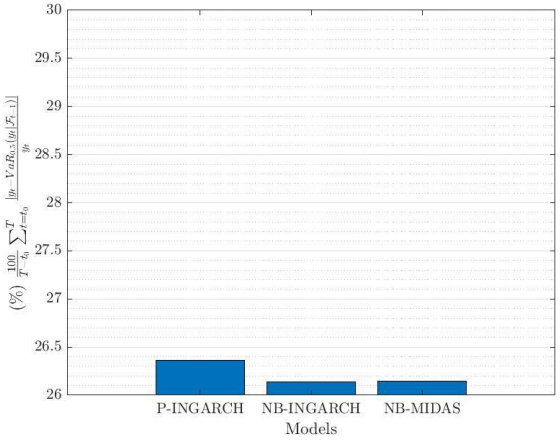

d) Mean Absolute Percentage Error (MAPE)

Note: Top figures gather different measures to analyse the forecasted distribution. Top left figure provides the PIT chart, whereas top right shows the log predictive score. Bottom figures focuses in the point estimates of the forecast, looking at the mean (RMSFE) and median (MAPE).

Panel D. OFC

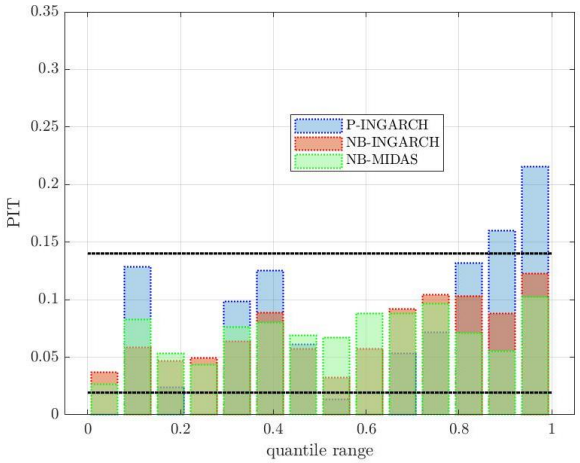

a) Probability Integral Transformation (PIT)

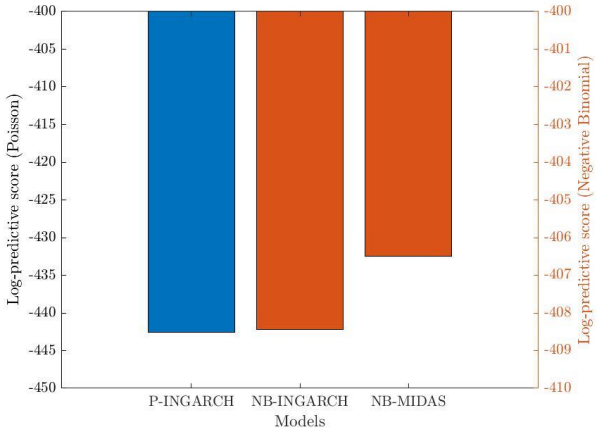

b) Log predictive score

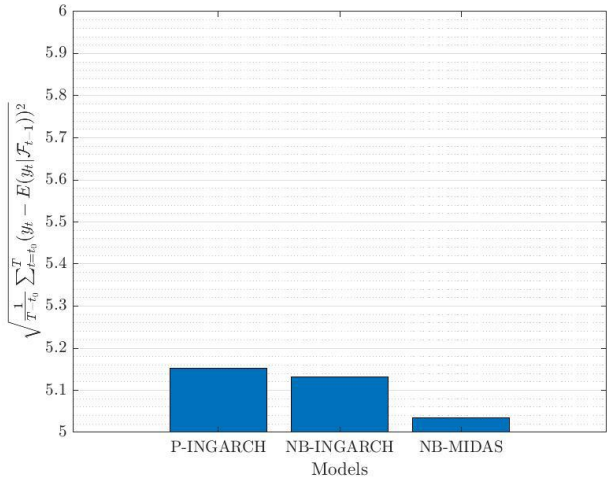

c) Root Mean Squared Forecast Error (RMSFE)

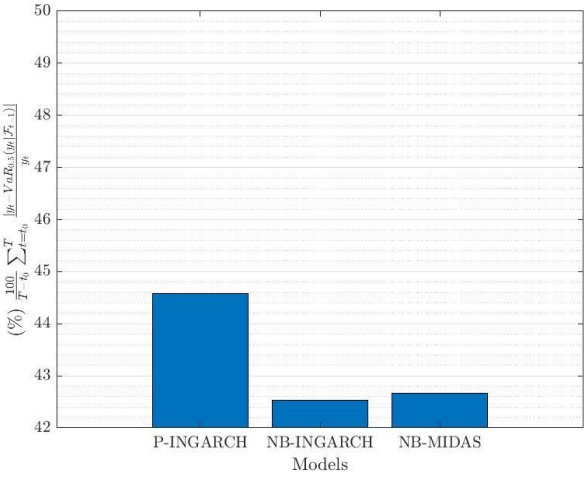

d) Mean Absolute Percentage Error (MAPE)

Note: Top figures gather different measures to analyse the forecasted distribution. Top left figure provides the PIT chart, whereas top right shows the log predictive score. Bottom figures focuses in the point estimates of the forecast, looking at the mean (RMSFE) and median (MAPE).

Panel E. Developed Asian

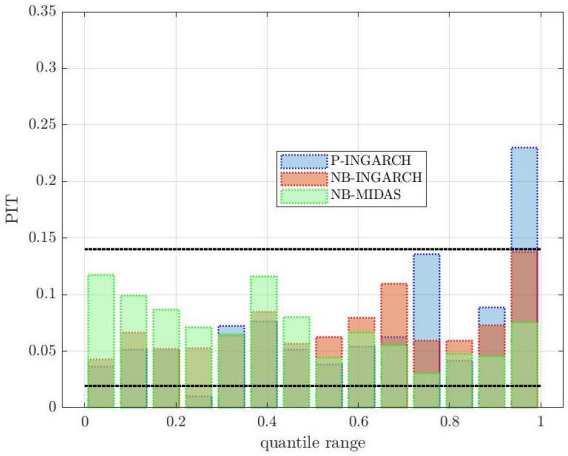

a) Probability Integral Transformation (PIT)

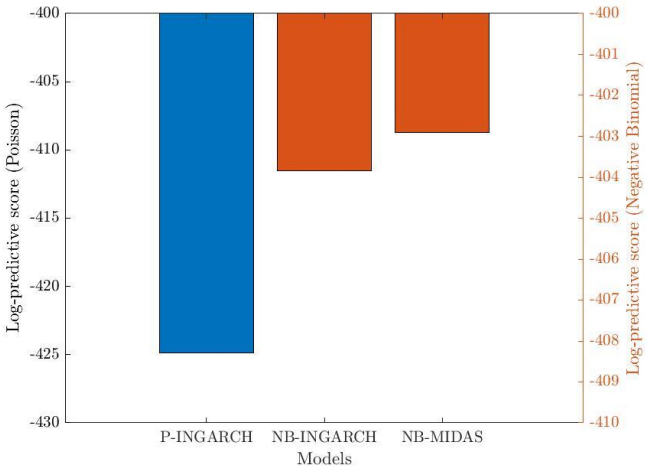

b) Log predictive score

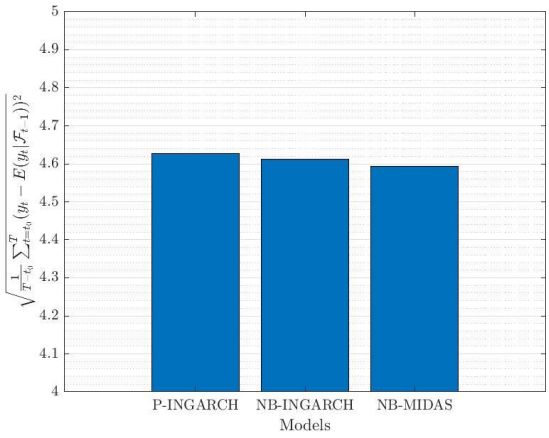

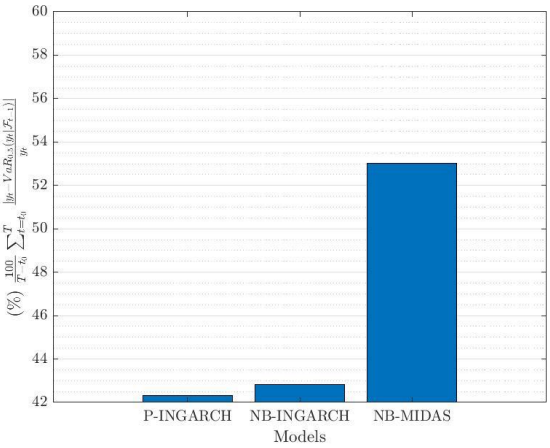

c) Root Mean Squared Forecast Error (RMSFE) d) Mean Absolute Percentage Error (MAPE)

Note: Top figures gather different measures to analyse the forecasted distribution. Top left figure provides the PIT chart, whereas top right shows the log predictive score. Bottom figures focuses in the point estimates of the forecast, looking at the mean (RMSFE) and median (MAPE).

Panel F. China

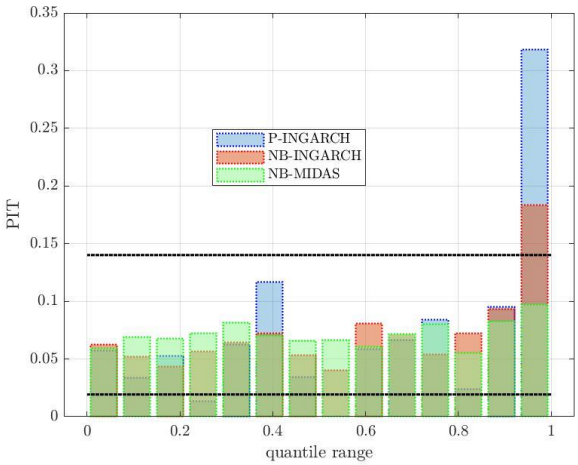

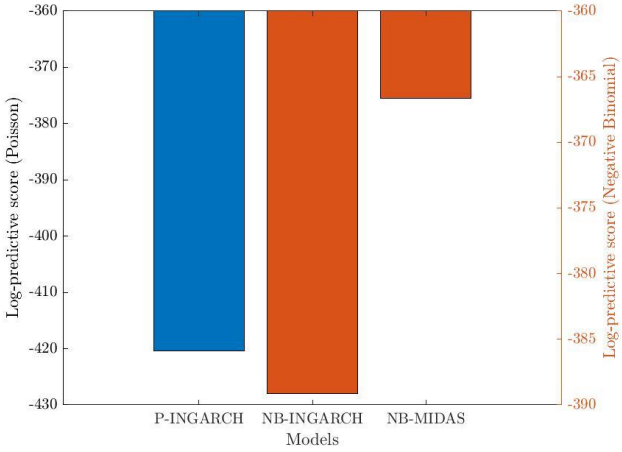

a) Probability Integral Transformation (PIT) b) Log predictive score

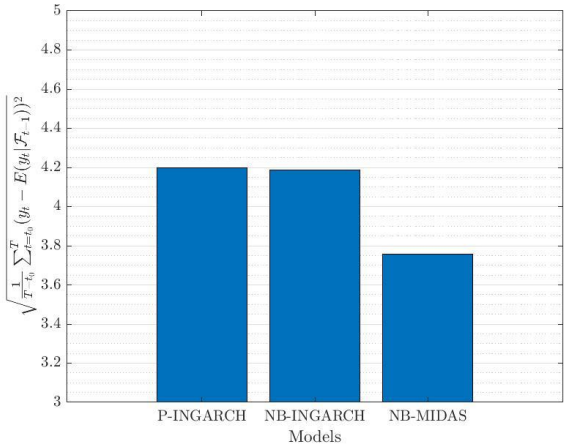

c) Root Mean Squared Forecast Error (RMSFE)

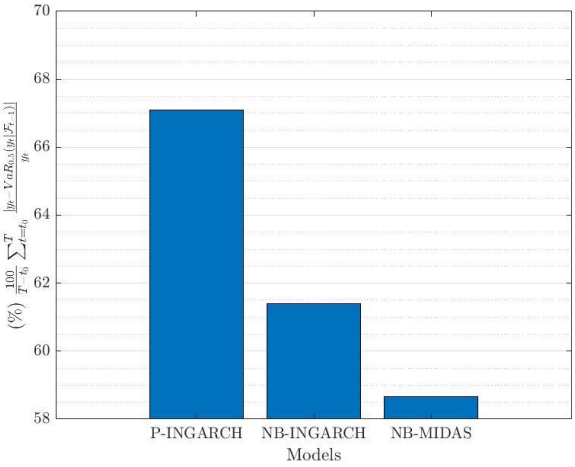

d) Mean Absolute Percentage Error (MAPE)

Note: Top figures gather different measures to analyse the forecasted distribution. Top left figure provides the PIT chart, whereas top right shows the log predictive score. Bottom figures focuses in the point estimates of the forecast, looking at the mean (RMSFE) and median (MAPE).

Figure 8: Forecast for the M&A deals for the period 03/2021-03/2022 at a regional level

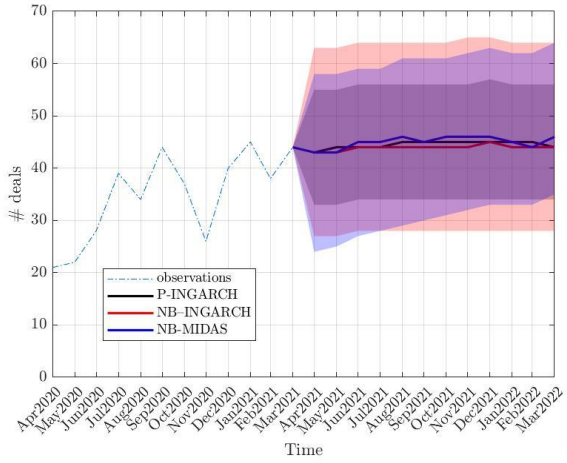

a) US and Canada

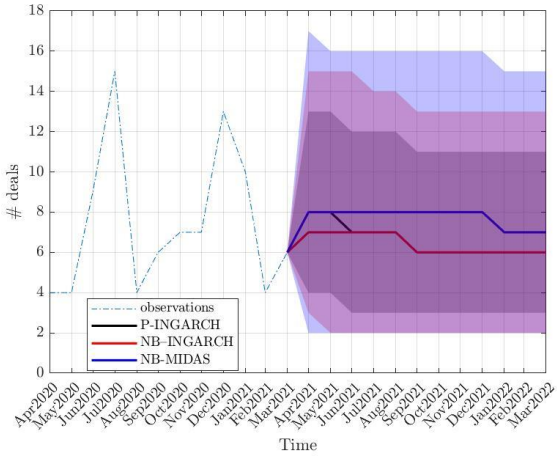

e) OFC

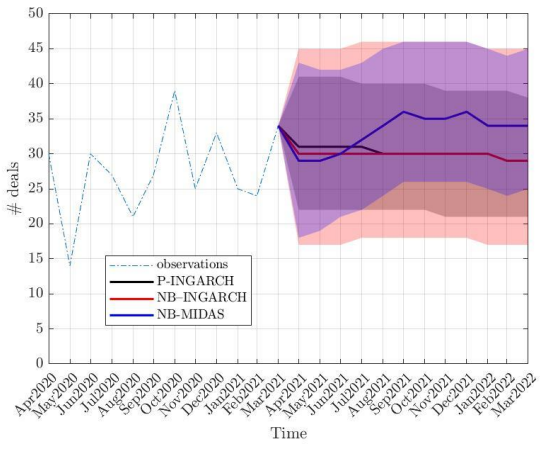

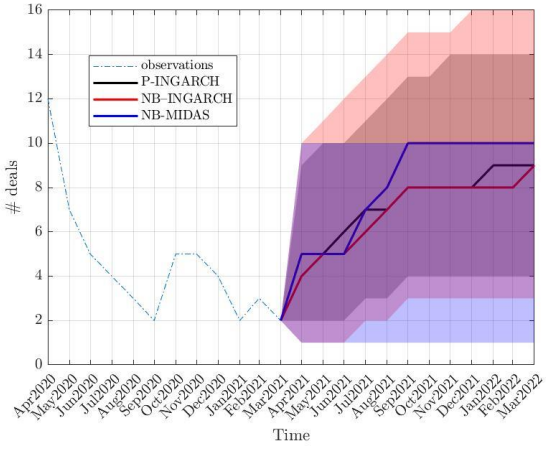

b) United Kingdom

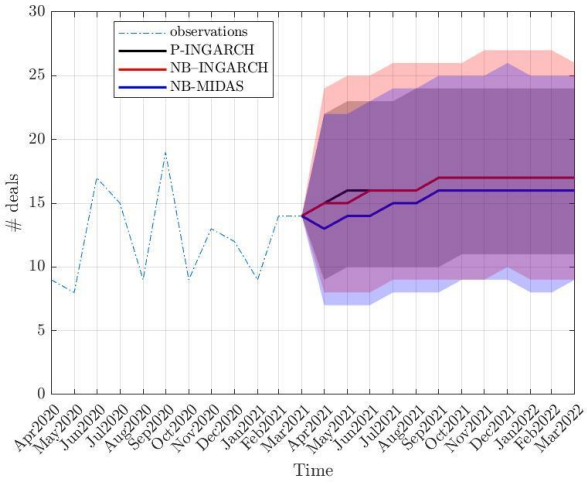

f) Developed Asia

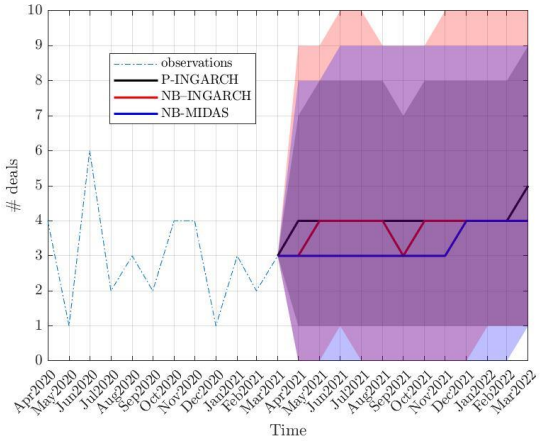

c) EFTA

g) China

Note: The area around the solid line indicate the 90% confidence interval whereas the solid line indicate the median.

Figure 9: Forecasted distribution and forecast performance for the sectorial M&A deals

Panel A. Manufacturing

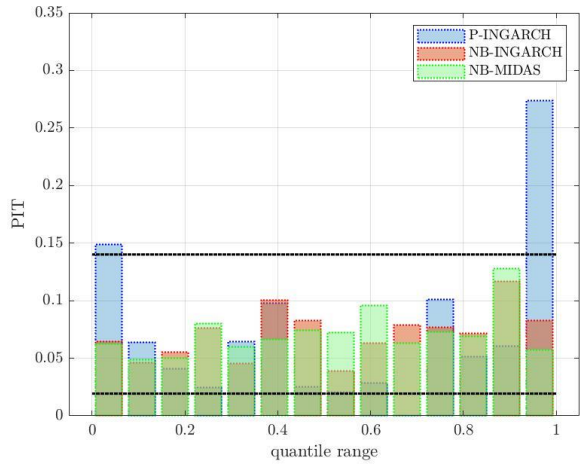

a) Probability Integral Transformation (PIT)

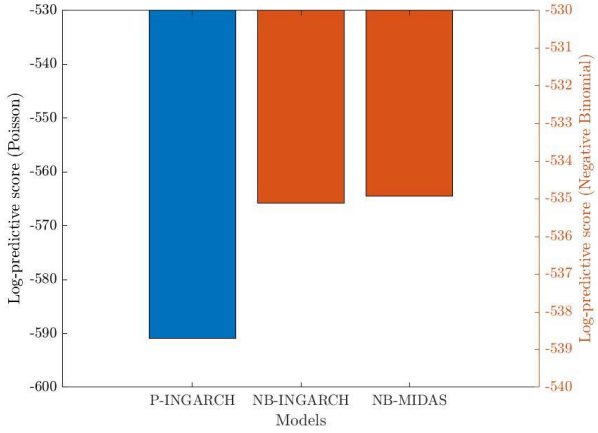

b) Log predictive score

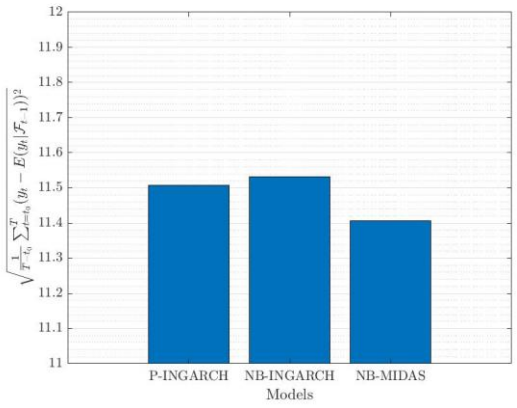

c) Root Mean Squared Forecast Error (RMSFE)

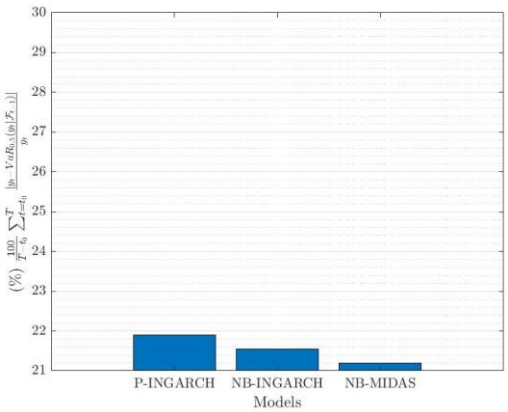

d) Mean Absolute Percentage Error (MAPE)

Note: Top figures gather different measures to analyse the forecasted distribution. Top left figure provides the PIT chart, whereas top right shows the log predictive score. Bottom figures focuses in the point estimates of the forecast, looking at the mean (RMSFE) and median (MAPE).

Panel B. Services

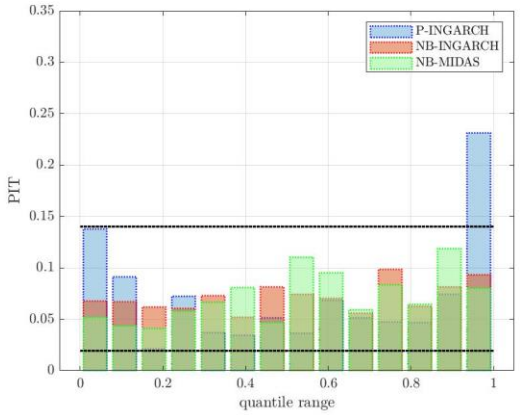

a) Probability Integral Transformation (PIT)

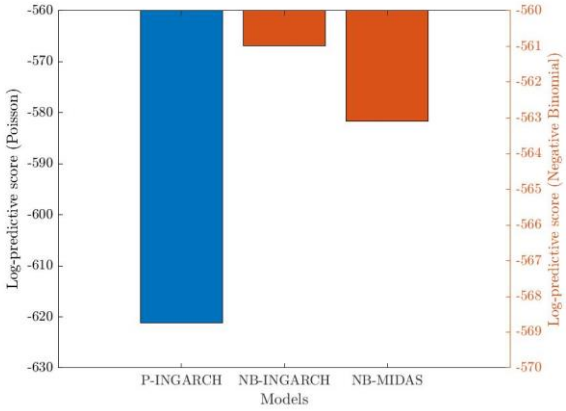

b) Log predictive score

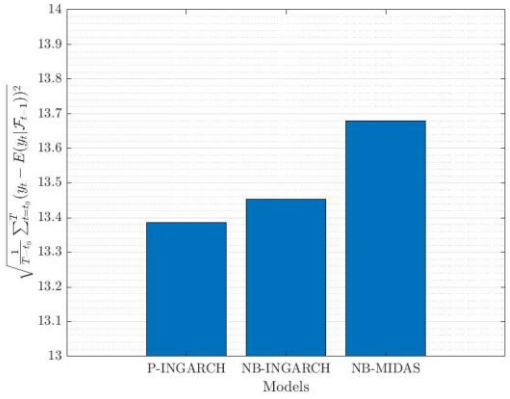

c) Root Mean Squared Forecast Error (RMSFE)

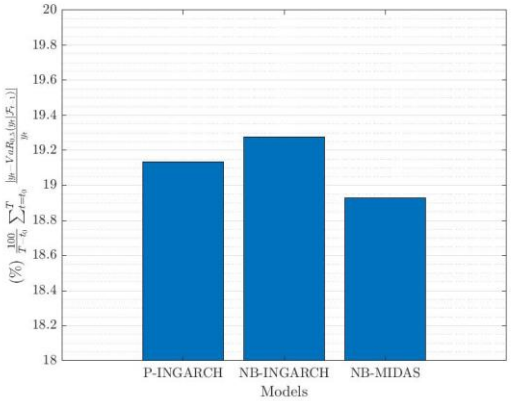

d) Mean Absolute Percentage Error (MAPE)

Note: Top figures gather different measures to analyse the forecasted distribution. Top left figure provides the PIT chart, whereas top right shows the log predictive score. Bottom figures focuses in the point estimates of the forecast, looking at the mean (RMSFE) and median (MAPE).

Panel C. Banking and Insurance

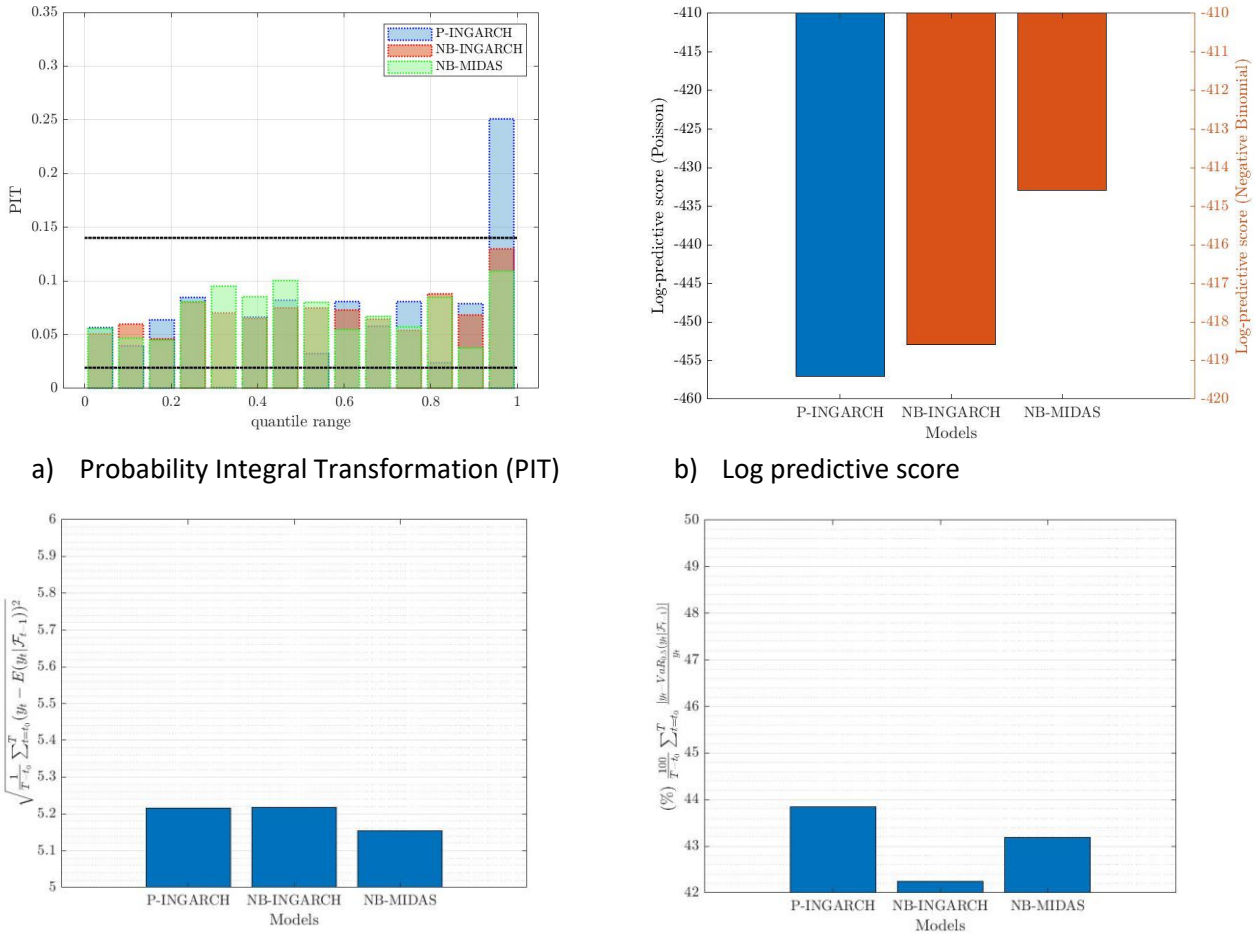

a) Probability Integral Transformation (PIT)

b) Log predictive score

c) Root Mean Squared Forecast Error (RMSFE)

d) Mean Absolute Percentage Error (MAPE)

Note: Top figures gather different measures to analyse the forecasted distribution. Top left figure provides the PIT chart, whereas top right shows the log predictive score. Bottom figures focuses in the point estimates of the forecast, looking at the mean (RMSFE) and median (MAPE).

Figure 10: Forecast for the M&A deals for the period 03/2021-03/2022 at a sectorial level

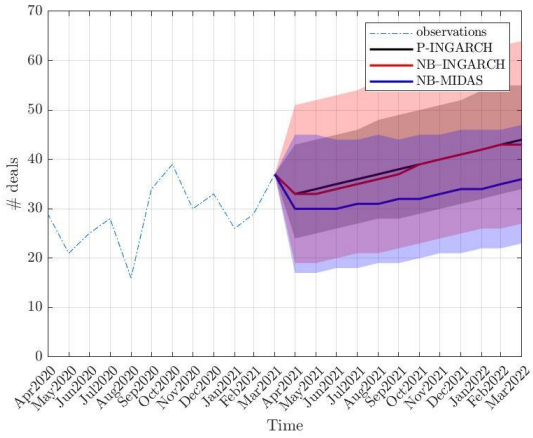

d) Manufacturing

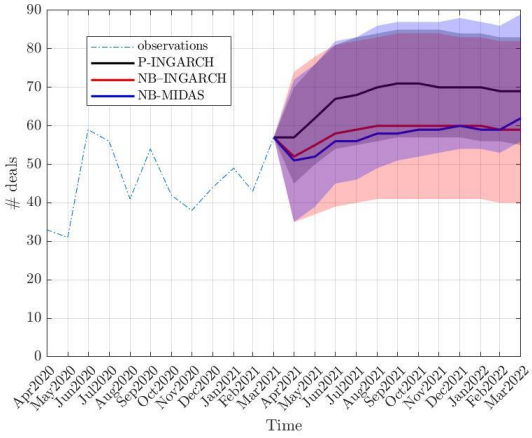

h) Services

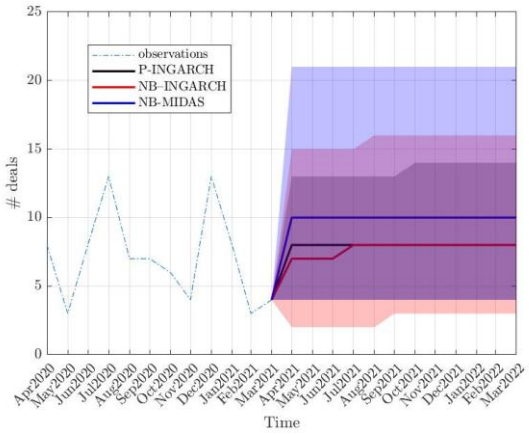

e) Banking and Insurance

Note: The area around the solid line indicate the 90% confidence interval whereas the solid line indicate the median.

Figure 11: Forecasted distribution and forecast performance for the M&A deals classified by their technological intensity of the manufacturing sector.

Panel A. Low and medium-low technology

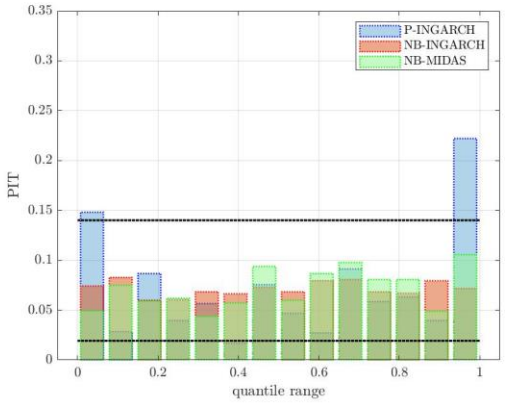

a) Probability Integral Transformation (PIT)

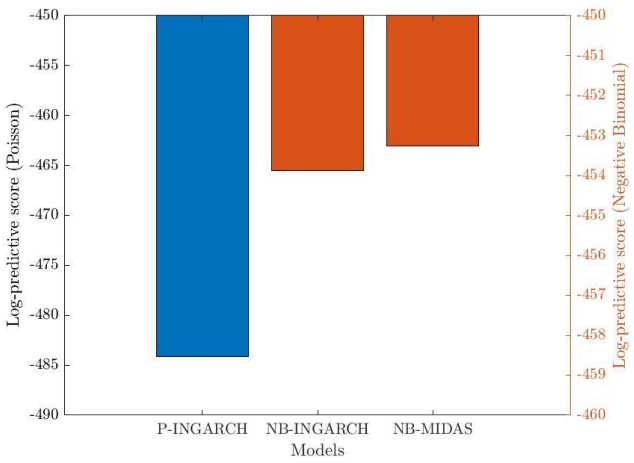

b) Log predictive score

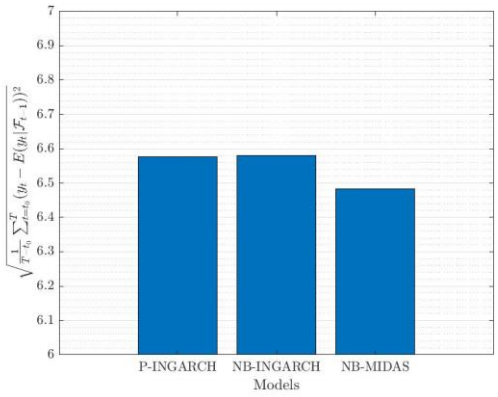

c) Root Mean Squared Forecast Error (RMSFE)

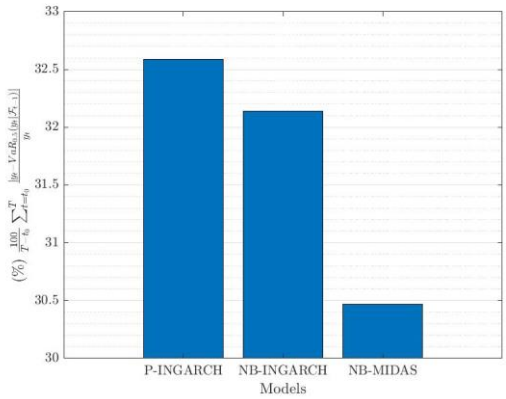

d) Mean Absolute Percentage Error (MAPE)

Note: Top figures gather different measures to analyse the forecasted distribution. Top left figure provides the PIT chart, whereas top right shows the log predictive score. Bottom figures focuses in the point estimates of the forecast, looking at the mean (RMSFE) and median (MAPE).

Panel B. High and medium-high technology

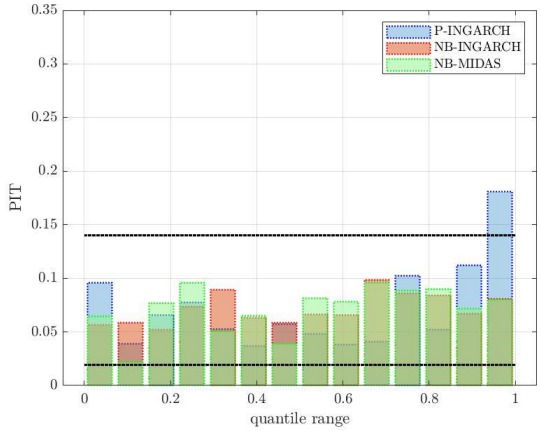

a) Probability Integral Transformation (PIT)

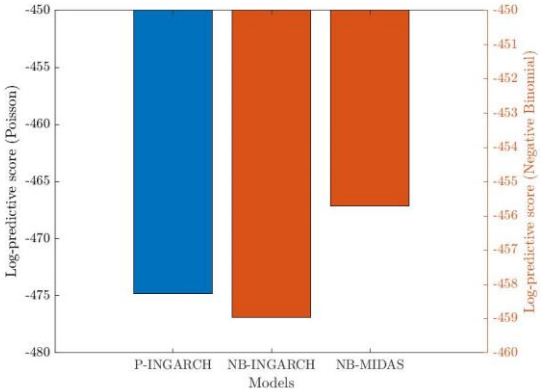

b) Log predictive score

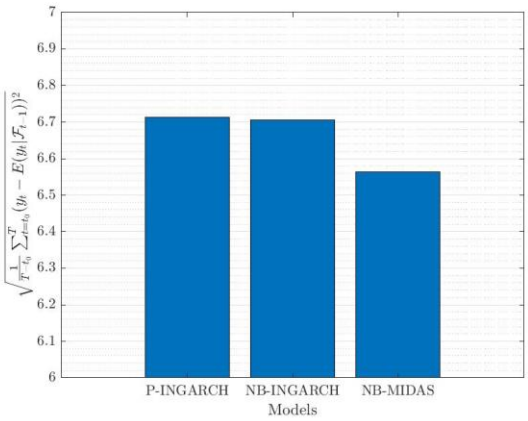

c) Root Mean Squared Forecast Error (RMSFE)

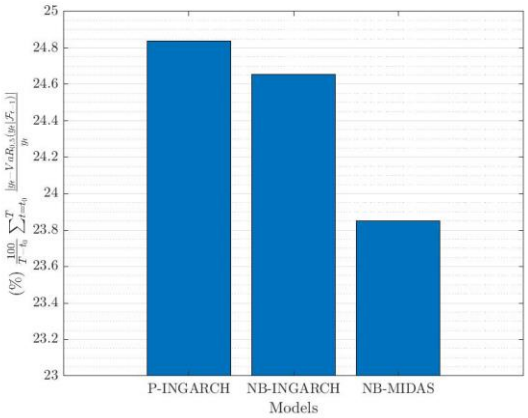

d) Mean Absolute Percentage Error (MAPE)

Note: Top figures gather different measures to analyse the forecasted distribution. Top left figure provides the PIT chart, whereas top right shows the log predictive score. Bottom figures focuses in the point estimates of the forecast, looking at the mean (RMSFE) and median (MAPE).

Figure 12: Forecast for the M&A deals for the period 03/2021-03/2022 at a technological intensity level

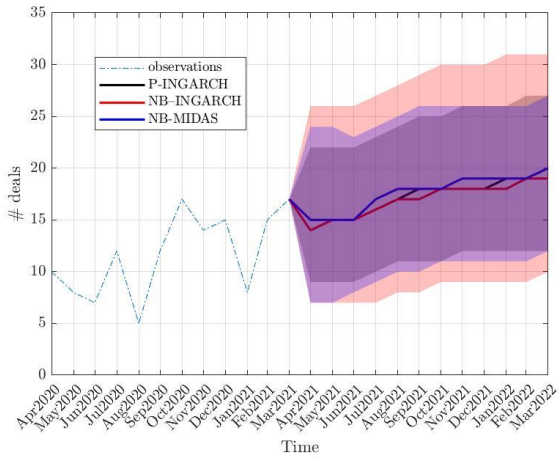

a) Low and medium-low technological intensity

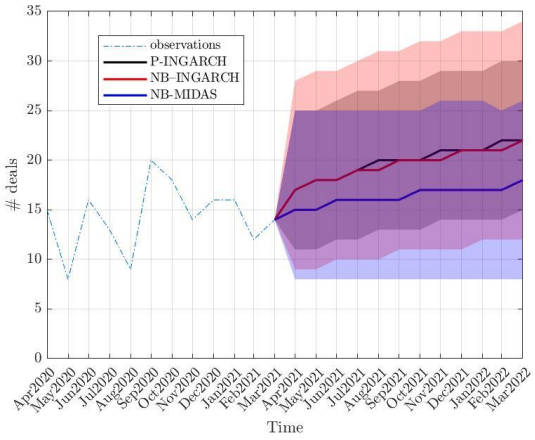

b) High and medium-high technological intensity

Note: The area around the solid line indicate the 90% confidence interval whereas the solid line indicate the median.

Appendix A: Poisson benchmark for count processes and INGARCH models

The description of the main features of count stochastic processes, i.e. the index of dispersion and the index of zeros, is based on a comparison with the characteristics of the Poisson distribution. The Poisson distribution has the distinctive feature of the equality between mean and variance, i.e. $\mu = \sigma^2$, which is known as equidispersion. The **index of dispersion** is the ratio between variance and mean, i.e.

$$I_{dispersion} = \frac{\sigma^2}{\mu},$$

which for the Poisson distribution has the unit value. If I>1, the distribution presents overdispersion, whereas if I<1, the distribution shows underdispersion. The number of M&A deals typically present very high monthly/daily volatility, hence overdispersion. The negative binomial, which has been widely used to model the number of M&A deals by the literature is an example of overdispersed distribution (Hijzen et al., 2008; Pozzolo & Focarelli, 2008).

Another feature of M&A deals is that their minimum value is zero and some zeros may actually occur in some of the periods observed, especially is deals are observed at high frequency (e.g. daily) or with breakdowns (e.g. by sector of investor country). The index employed to describe this statistical property in a count process is known as the **zero index**, which represents the probability of observing a zero in the process (Weiss, 2017). This index is a measure of the left tail skewness, which in count data has a lower bound at zero, and is a function of the probability of observing a zero scaled by the mean of the process, i.e.

$$I_{zero} = 1 + \frac{P(y = 0)}{\mu},$$

For the Poisson the value is zero, whereas $I_{zero} > 0$ $(I_{zero} < 0)$ indicates zero inflation (deflation).

INGARCH models

INGARCH models are the integer-valued counterpart to the conventional GARCH model (Weiss, 2017), where the "IN" indicates the integer-valued structure of the data (Weiß, 2009).The inclusion of exogenous variables in the model deals to an extension of the standard model known as INGARCHX model (Agosto et al., 2016, Agosto and Ahelegbey, 2020). The INGARCH models together with the use of a Poisson distribution for the autoregressive process is the main benchmark for count processes. This methodology is also known as autoregressive conditional Poisson (ACP) model (Heinen, 2011a) or Poisson autoregressive (PAR) model (Fokianos et al., 2009). The INGARCH model allows for modelling parsimoniously a long memory process, i.e. the case in which the conditional mean depends on the whole history of the process (Fokianos, 2011).

This type of model has been widely employed to fix the evolution of different count time series like COVID-19 contagion dynamics (Agosto and Giudici, 2020). The PAR assumes that the conditional mean $E(Y_t|F_{t-1})$ shows a GARCH-type dynamic, as follows:

$$E(Y_t|F_{t-1}) = \mu_t = \omega + \sum_{i=1}^{Q} \alpha_i Y_{t-i} + \sum_{j=1}^{P} \beta_j \lambda_{t-j} + \boldsymbol{X}_{t-1}\boldsymbol{\gamma} \qquad \text{(A.1)}$$

where $\sum_{i=1}^{Q} \alpha_i + \sum_{j=1}^{P} \beta_j \leq 1$, $\alpha, \beta \in (0,1)$, $\omega \geq 0$ and $\boldsymbol{X}'_{t-1}$ is a column vector of size K of exogenous variables which are known at t-1, while γ is a column vector of length K reporting the coefficients of the exogenous variables to forecast future values of the conditional mean.

Ferland et al.(2006) and Heinen (2011b) study the particular case of INGARCH(1,1) Note that the distribution is conditional equidispersed but unconditional overdispersed. For instance, let us consider the INGARCH(1,1), we have $E(Y_t|Y_{t-1}) = \lambda_t = Var(Y_t|Y_{t-1})$, whereas using the Law of Iterated Expectation we get $E(Y_t) = E\big(E(Y_t|Y_{t-1})\big) = E(\lambda_t) = \frac{\omega}{1-\alpha-\beta}$, and using the Law of the Total Variance $Var(Y_t) = E\big(Var(Y_t|Y_{t-1})\big) + Var\big(E(Y_t|Y_{t-1})\big) = E(\lambda_t) + Var(\lambda_t) > E(\lambda_t)$ and $Var(\lambda_t) = \frac{1-(\alpha+\beta)^2+\alpha^2}{1-(\alpha+\beta)^2} E(\lambda_t)$.

The main drawback of the PAR model is the assumption of equal-dispersed distribution, i.e. the Poisson distribution assumes that the conditional mean is equal to the conditional variance,[19] hence $E(Y_t|F_{t-1}) = Var(Y_t|F_{t-1})$. Conversely, the variance of a count process could be much higher than its mean. To capture this feature, the dispersed INGARCH model, also known as DIN-INGARCH, defines the conditional variance as a factor of the conditional mean, i.e. $E(Y_t|F_{t-1}) = \kappa Var(Y_t|F_{t-1})$, where $\kappa > 1$ to reflect overdispersion. Xu et al. (2012) propose the use of the negative binomial distribution to capture the conditional overdispersion, where $Y_t|F_{t-1} \sim NB(\eta_t, \pi)$, and the conditional mean $E(Y_t|F_{t-1}) = \frac{\eta_t(1-\pi)}{\pi}$ follows Equation (1), while the conditional variance is defined as $Var(Y_t|F_{t-1}) = \frac{\eta_t(1-\pi)}{\pi^2}$. Consequently, the DIN-INGARCH model under the negative binomial distribution proposed by Xu et al. (2012) has $\kappa = \frac{1}{\pi}$, where $\pi \in (0,1)$ and the model converges to the Poisson distribution when $\pi \to 1$ and $\eta_t \to \infty$ such that $\eta_t(1-\pi) \to \lambda_t$. Zhu (2012) proposes a DIN-INGARCH model under the assumption of a

[19] The INGARCH model already introduces an unconditioned overdispersion. In particular, $\sigma^2 = \frac{1-(\alpha-\beta)^2+\alpha^2}{1-(\alpha+\beta)^2}\mu$ (Weiss 2017, pp. 76). However, the conditional moments are still equal-dispersed under the Poisson distribution, i.e. $\sigma_t^2 = \mu_t$.

Generalized Poisson distribution, i.e. $GP(\theta, \lambda_t(1-\theta))$ The Generalized Poisson distribution reflects overdispersion in the data through the extra parameter $\theta \in (0,1)$, which defines the dispersion index, i.e. $I_{dispersion} = \frac{1}{1-\theta^2}$. Note that when $\theta \to 0$ we obtain the Poisson distribution.

GETTING IN TOUCH WITH THE EU

In person

All over the European Union there are hundreds of Europe Direct centres. You can find the address of the centre nearest you online (european-union.europa.eu/contact-eu/meet-us_en).

On the phone or in writing

Europe Direct is a service that answers your questions about the European Union. You can contact this service:

— by freephone: 00 800 6 7 8 9 10 11 (certain operators may charge for these calls),

— at the following standard number: +32 22999696,

— via the following form: european-union.europa.eu/contact-eu/write-us_en.

FINDING INFORMATION ABOUT THE EU

Online

Information about the European Union in all the official languages of the EU is available on the Europa website (european-union.europa.eu).

EU publications

You can view or order EU publications at op.europa.eu/en/publications. Multiple copies of free publications can be obtained by contacting Europe Direct or your local documentation centre (european-union.europa.eu/contact-eu/meet-us_en).

EU law and related documents

For access to legal information from the EU, including all EU law since 1951 in all the official language versions, go to EUR-Lex (eur-lex.europa.eu).

Open data from the EU

The portal data.europa.eu provides access to open datasets from the EU institutions, bodies and agencies. These can be downloaded and reused for free, for both commercial and non-commercial purposes. The portal also provides access to a wealth of datasets from European countries.

The European Commission's science and knowledge service

Joint Research Centre

JRC Mission

As the science and knowledge service of the European Commission, the Joint Research Centre's mission is to support EU policies with independent evidence throughout the whole policy cycle.

EU Science Hub
joint-research-centre.ec.europa.eu

@EU_ScienceHub

EU Science Hub - Joint Research Centre

EU Science, Research and Innovation

EU Science Hub

EU Science